Neutrino process for ^{10}Be production with updated relevant nuclear reactions

Myung-Ki Cheoun (천명기, 千明起)
(**Soongsil University**, **OMEG Institute & Dept. of Physics**, Seoul, Korea)

Heamin Ko, T. Hayakawa, G. Mathews, T. Kajino …

Astrophysical neutrinos and the origin of the elements
Week 2 (Embedded Workshop) July 24028, 2023, INT U. of Washington

Contents

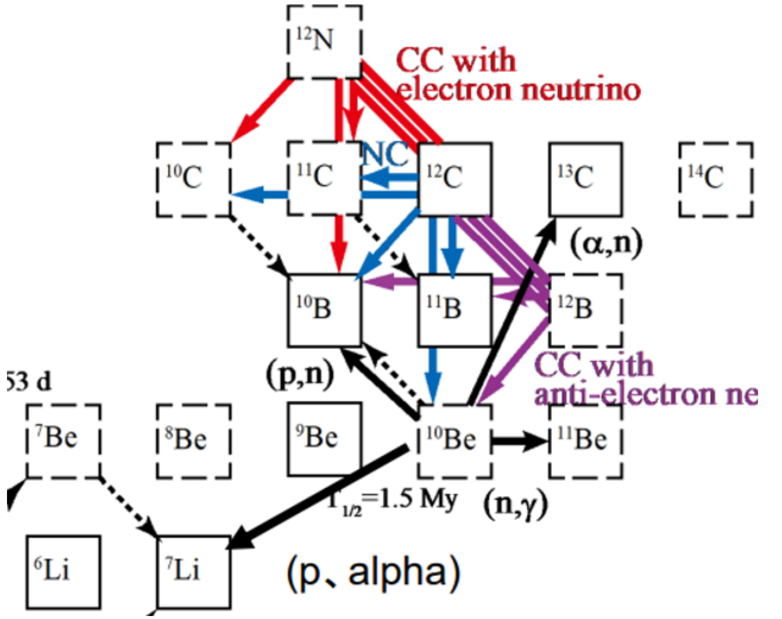

1. Motivation of the Neutrino-process

2. Cosmological Origin of ^{10}Be (Short-lived Radioactive Nucleus)

2-1. Ratio of $^{10}Be/^{9}Be$ by the Neutrino-process

2-2. Relevant Nuclear Reactions for ^{10}Be Production

3. Summary and Conclusion

Neutrino Process in CCSN Explosion

Why neutrino process in SN?

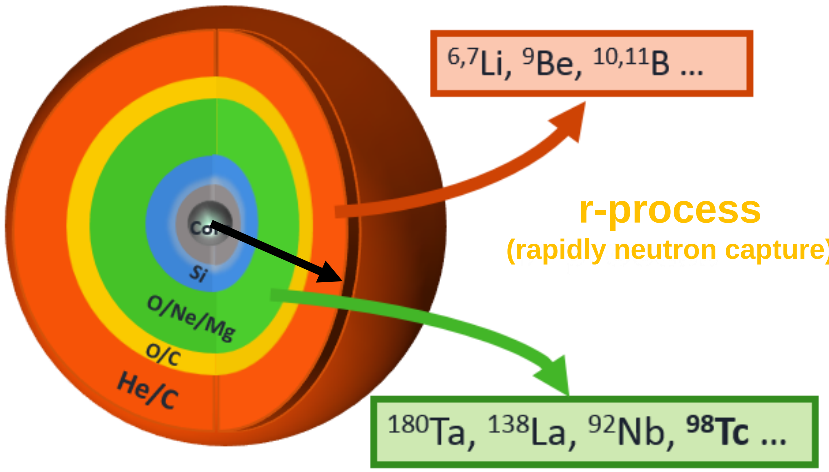

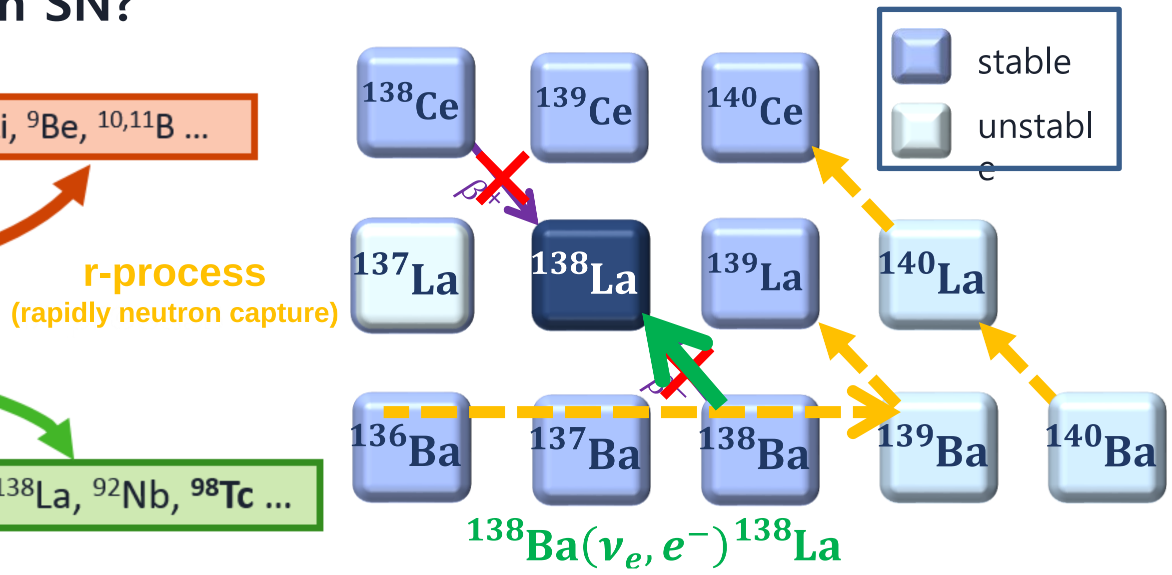

Total Hamiltonian for neutrino propagation in matter

$$H_{\text{total}} = H_{\text{Vacuum}} + V_{\text{matter}} + V_{\text{self}}$$

- Vacuum and matter term

$$H_{\text{Vacuum}} = \frac{1}{2\epsilon_\nu} U \begin{pmatrix} 0 & 0 & 0 \\ 0 & \Delta m_{21}^2 & 0 \\ 0 & 0 & \Delta m_{31}^2 \end{pmatrix} U^\dagger, \qquad V_{\text{matter}}(r, E, \theta_p) = \begin{pmatrix} \pm\sqrt{2} G_F n_e & 0 & 0 \\ 0 & 0 & 0 \\ 0 & 0 & 0 \end{pmatrix}$$

Unitary mixing PMNS matrix

$$U = \begin{pmatrix} c_{12}c_{13} & s_{12}c_{13} & s_{13} \\ -s_{12}c_{23} - c_{12}s_{23}s_{13} & c_{12}c_{23} - s_{12}s_{23}s_{13} & s_{23}c_{13} \\ s_{12}s_{23} - c_{12}c_{23}s_{13} & -c_{12}s_{23} - s_{12}c_{23}s_{13} & c_{23}c_{13} \end{pmatrix}$$

Neutrino parameters
$\theta_{12} = 33.8°, \theta_{23} = 45°, \theta_{13} = 9.2°$
$\Delta m_{21}^2 = 7.54 \times 10^{-5}\ [\text{eV}^2],\ |\Delta m_{31}^2| \approx 2.4 \times 10^{-3}\ [\text{eV}^2]$

K. A. Olive, *et al*. [Particle Data Group], Chin. Phys. C 38, 090001 (2014).

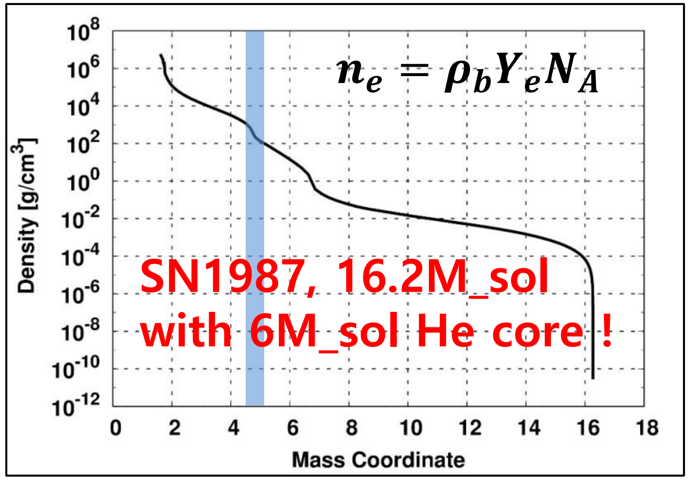

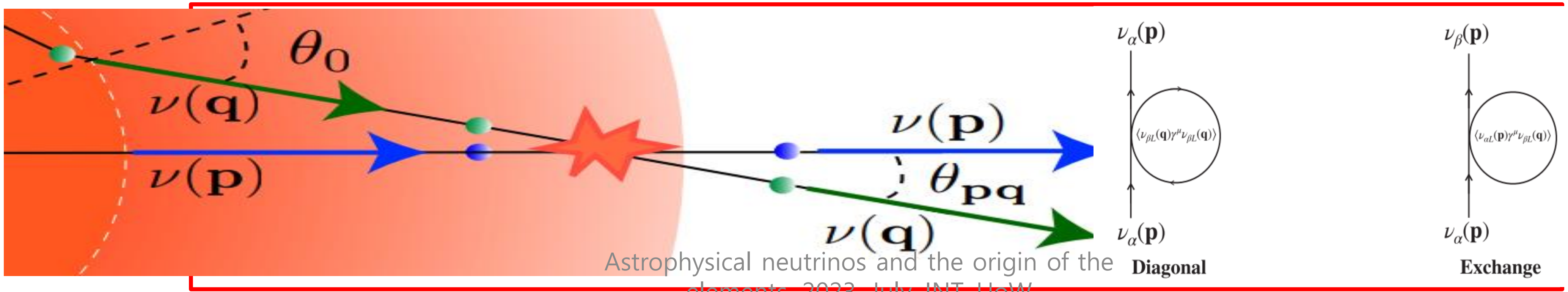

Self-Interaction effects on the **Neutrino Flux**

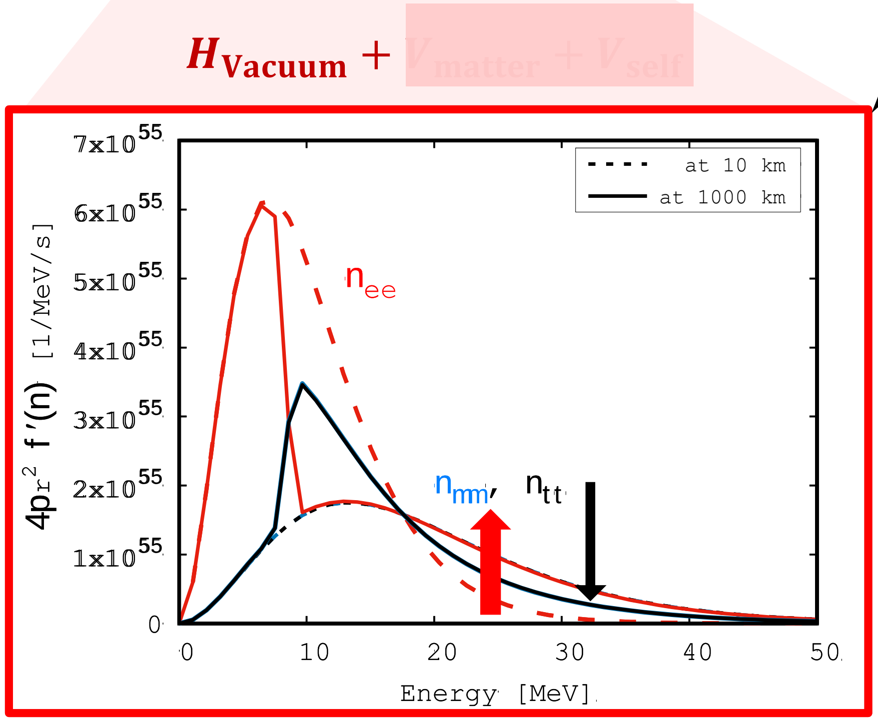

H. Sasaki, *et al.*(NAOJ) in private communication (2018)

Inverted mass hierarchy (IH)

The differential neutrino flux with neutrino flavor α

$$\phi'(t,r;\epsilon_\nu,T_\alpha) \equiv \frac{d}{d\epsilon_\nu}\phi(t,r;\epsilon_\nu,T_\alpha)$$

$$= \frac{L_\nu}{4\pi r^2}\frac{1}{\langle\epsilon_\nu\rangle}\frac{\epsilon_\nu^2}{\exp(\epsilon_\nu/T_\alpha)+1}\langle\rho_{\alpha\alpha}\rangle$$

The neutrino temperatures are

$$T_{\nu_e} = 3.2,\ T_{\bar{\nu}_e} = 5 \text{ and } T_{\nu_x} = 6\ [\mathrm{MeV}/k_B]$$

T. Yoshida, *et al.*, Astrophys. J. 686, 448 (2008)

- ✓ Initially we assume Fermi-Dirac distribution for neutrino spectra (**EQ luminosity**).
- ✓ In the case of normal mass hierarchy, the SI effect is suppressed.
- ✓ For anti-neutrino, similar effects are found.
- ✓ **For the luminosity we use other numerical luminosity by the neutrino transport simulation (NEQ Luminosity).**

Neutrino Luminosity in CCSN Explosion

J. Phys. G: Nucl. Part. Phys. **45** (2018) 104001 E O'Connor *et al*

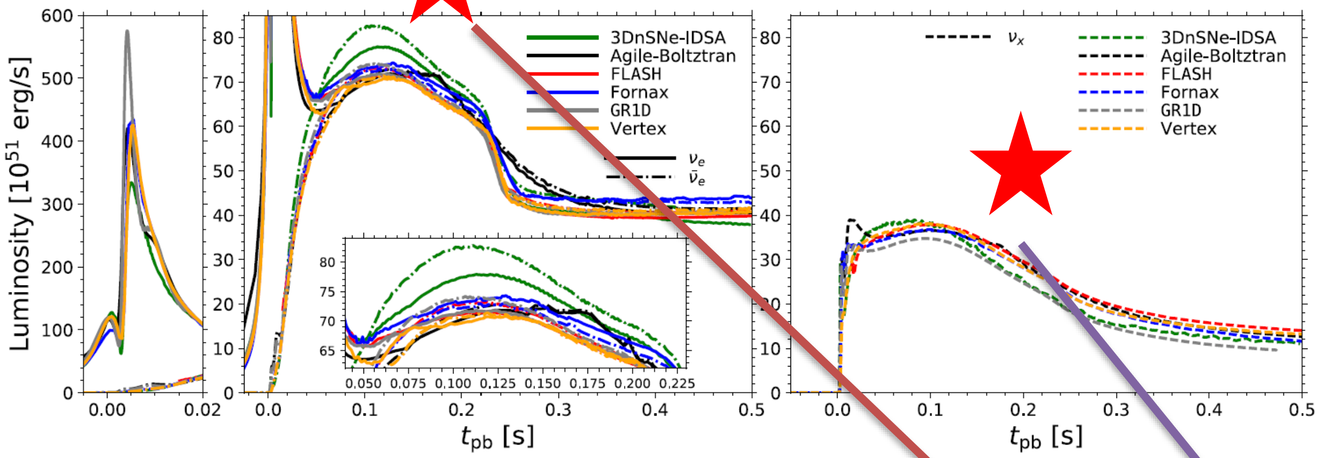

Figure 3. Neutrino luminosities as a function of postbounce time. In the left panels we show electron-type neutrino luminosities (solid lines show electron neutrinos while dashed–dotted lines show electron antineutrinos) and in the right panel we show the characteristic heavy-lepton neutrino luminosity (dashed line). For clarity, we show an inset to highlight the early accretion epoch for the elec... to show the neutronization burst. Some curves have be... remove noise and improve clarity.

3.1. 3DnSNe-IDSA

Contributors: *Tomoya Takiwaki, Kei Kotake*

3.2. AGILE-BOLTZTRAN

Contributors: *Tobias Fischer, Eric Lentz, Matthias Liebendörfer, Bronson Messer, Anthony Mezzacappa* The radiation-hydrodynamics module AGILE is based on the spherically-sym-

3.3. FLASH-M1

Contributors: *Evan O'Connor, Sean Couch*

3.4. FORNAX

Contributors: *Adam Burrows, David Vartanyan*

3.5. GR1D

Contributors: *Evan O'Connor*

3.6. PROMETHEUS-VERTEX

Contributors: *Robert Bollig, Hans-Thomas Janka*

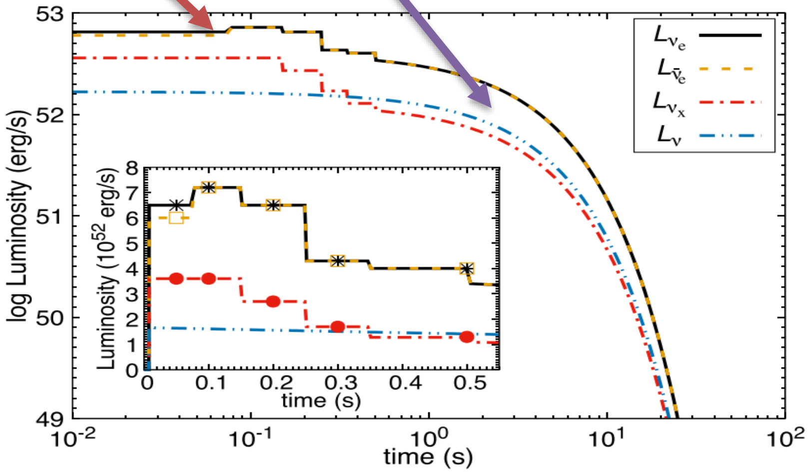

Figure 10. The neutrino luminosities for each flavor: ν_e, $\bar{\nu}_e$, and $\nu_x (= \nu_\mu, \nu_\tau, \bar{\nu}_\mu$ and $\bar{\nu}_\tau)$ in the region of $M_r \sim 1.6 M_\odot$(corresponding to $r \sim 2300$ km). The inset shows an enlarged figure of the *x*- and *y*-axes. The yellow line denotes the luminosity calculated by Equation (14) and the others are adopted from Table 2.

Input Data Model for neutrino-process for CCSN Explosion

JINA REALIB

Modified (n,g) Reactions

QRPA & Branching Ratios

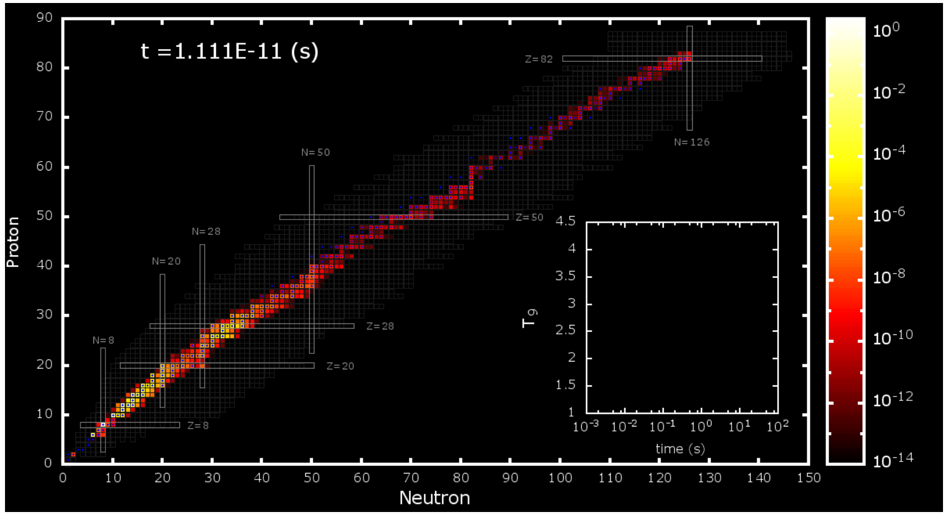

Numerical results for elements abundances

1987 SN model

Pre-supernova Model

Hydrodynamics Model: HCK18, KCK19

★ Modified Neutrino Flux by Self-interaction : w/ and w.o/

★ Neutrino Luminosity : EQ and NEQ

Mass Hierarchy : NH and IH

Introduction

Hydrodynamics for the **Neutrino Process in CCSN Explosion**

THE ASTROPHYSICAL JOURNAL, 937:116 (37pp), 2022 October 1 Ko et al.

SN1987A has been verified as an explosion of a blue supergiant star, Sk–69 202, in the Large Magellanic Cloud, which has been estimated to have had a (19 ± 3) solar mass ($M_\odot$) in the main sequence, following the analysis of the light curve, with the metallicity being given as $Z \sim Z_\odot/4$ (Woosley 1988). Among the various explosive models satisfying the given conditions (Janka 2012), for the pre-SN model we adopt the initial density and temperature profiles from Kikuchi et al. (2015), whose results are similar to those of Shigeyama & Nomoto (1990). For the hydrodynamics models, we exploit the model in Kusakabe et al. (2019), based on the blcode,[11] with an explosion energy of 10^{51} erg. To discuss the effects of the hydrodynamics models, we introduce another model, used in Hayakawa et al. (2018), which was gleaned from the pre-SN model of Blinnikov et al. (2000), and has also been used in Hayakawa et al. (2013; 2018), and Ko et al. (2020). We call the former and latter models the "KCK19" (Kusakabe et al. 2019) and "HKC18" (Blinnikov et al. 2000) models, respectively. The HKC18 model turns out to have an inconsistency with the adopted pre-SN model. A detailed explanation of this inconsistency between the hydrodynamics model and pre-SN model is given in Section 5.

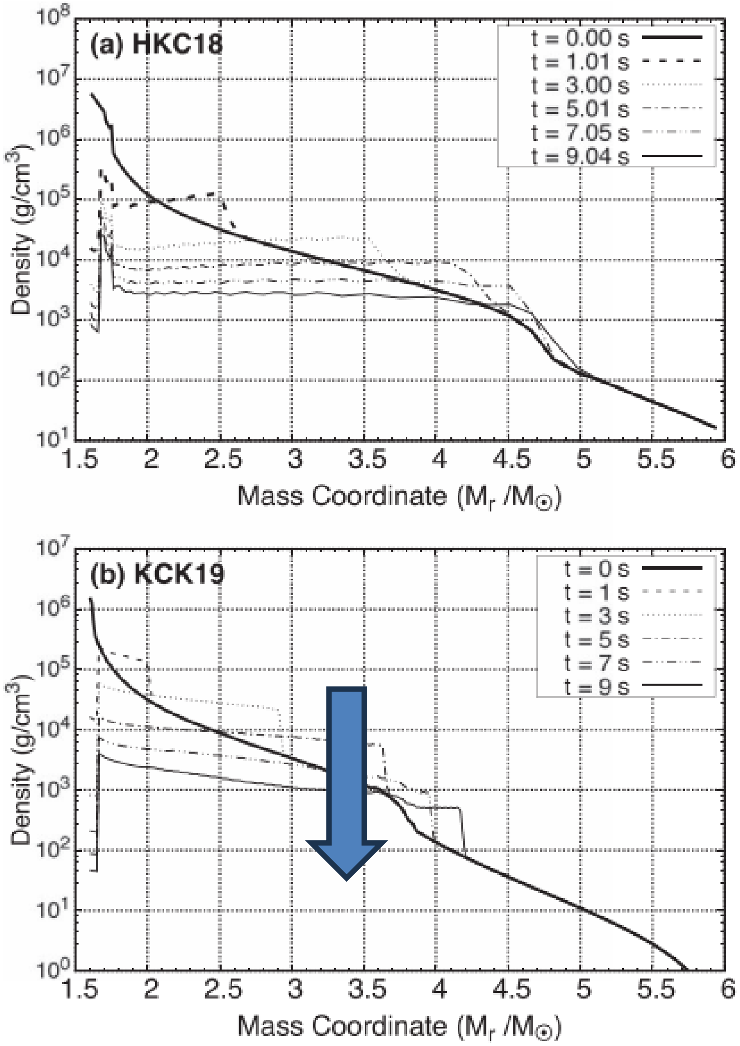

Figure 1. Time-evolving density profiles in the Lagrange mass coordinate. The upper and lower panels show the HKC18 (Blinnikov et al. 2000) and KCK19 (Kusakabe et al. 2019) hydrodynamics models, respectively. The time range is taken from about 0 to 7 s.

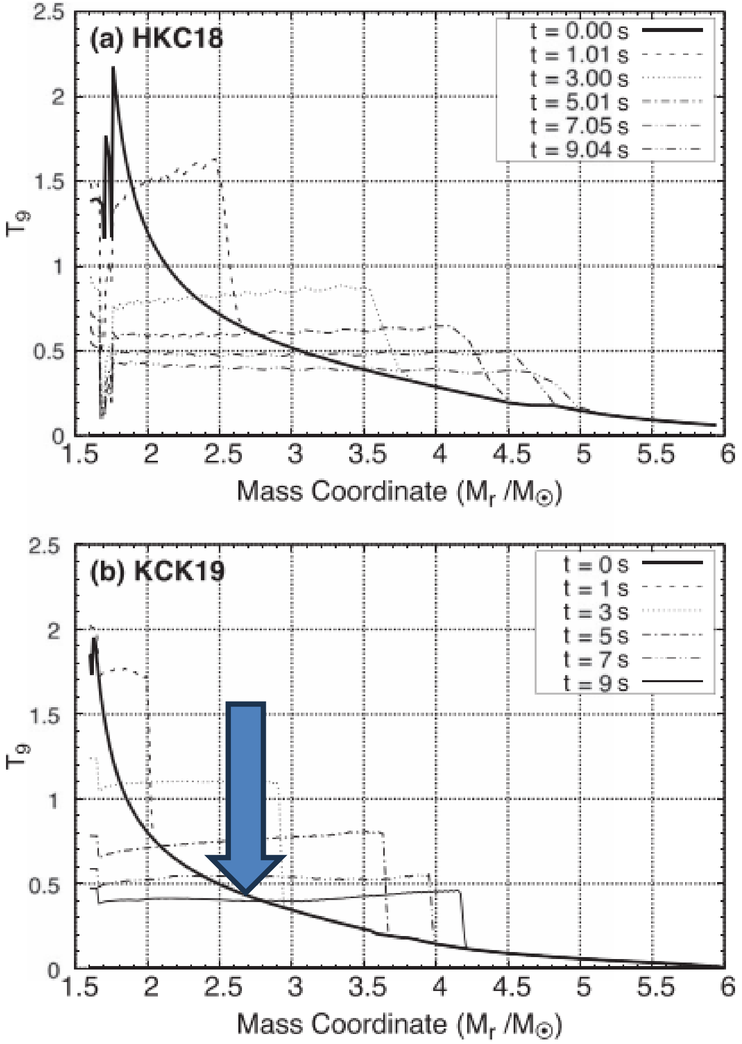

Figure 2. Time-evolving temperature profiles as a function of the Lagrange mass coordinate. The upper and lower panels show the same models as in Figure 1, respectively. The temperature unit is taken as $T_9 = T/(10^9\ \mathrm{K})$.

Introduction Nuclear Abundance Ratio in the neutrino-process

Hydrodynamics : HKC18 and KCK19 / Luminosity : EQ and NEQ
Neutrino Self Interaction : FD and SI / Mass Hierarchy : NH and IH

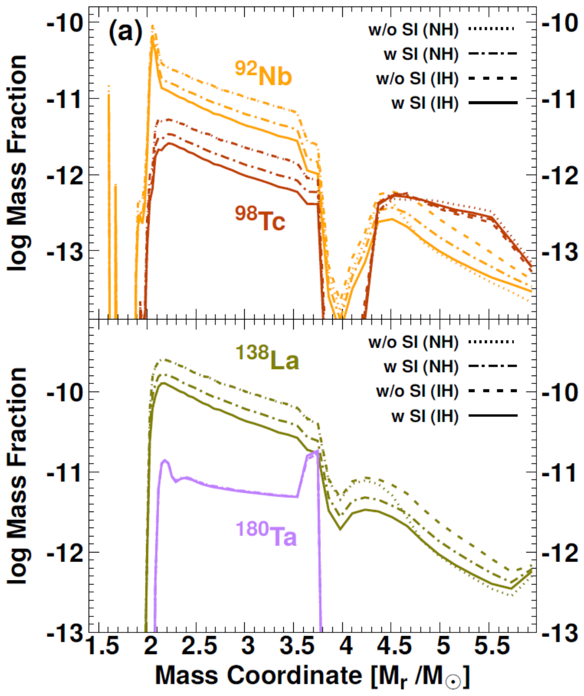

Table 4. Integrated masses of the nuclei after 50 s in the mass range, M_r = 1.6–6 ($M_\odot$). We used two hydrodynamics models (HKC18 and KCK19), two luminosity models (EQ and NEQ) and two cases without the ν−SI (FD) and with the ν−SI (SI) for the NH and IH case, by which the results for twelve different cases are tabulated. The last two results are quoted from our previous results. See texts for the details.

	Mass Hierarchy	^{7}Li	^{7}Be	^{11}B	^{11}C	^{92}Nb	^{98}Tc	^{138}La	^{180}Ta	Yield ratio	PF ratio
		(10^{-7} $M_\odot$)				(10^{-12} $M_\odot$)		(10^{-11} $M_\odot$)		N(^{7}Li)/N(^{11}B)	^{138}La/^{11}B
FD EQ (HKC18)	NH	1.256	4.953	5.576	2.048	4.903	1.048	3.395	0.845	1.280	0.1288
	IH	1.496	1.461	7.141	1.218	4.760	1.112	3.267	0.843	0.556	0.1130
FD EQ (KCK19)	NH	0.861	2.428	2.480	2.139	4.551	1.180	3.760	1.016	1.119	0.2354
	IH	1.017	0.936	3.099	0.883	4.226	1.218	3.436	1.012	0.771	0.2495
FD EQ Shock (KCK19)	NH	0.861	1.904	2.546	1.701	4.973	1.271	4.164	1.017	1.023	0.2835
	IH	0.949	1.027	2.922	0.937	4.271	1.215	3.485	1.012	0.805	0.2611
SI EQ^a (KCK19)	NH	0.861	2.428	2.480	2.139	4.551	1.180	3.760	1.016	1.119	0.2354
	IH	0.920	2.057	2.852	3.874	15.07	3.259	13.58	1.052	0.695	0.5838
SI NEQ (KCK19)	NH	1.132	1.601	4.276	4.920	16.44	3.559	15.19	1.295	0.467	0.4776
	IH	1.261	1.206	4.623	4.283	12.29	2.854	11.31	1.281	0.435	0.3672
FD NEQ (KCK19)	NH	1.483	0.841	5.407	5.258	25.44	5.367	23.14	1.323	0.342	0.6274
	IH	0.959	2.303	3.946	6.566	26.15	5.302	23.94	1.331	0.488	0.6585
SI NEQ Ko et al. (2020) (HKC18)	NH	1.643	3.347	9.332	6.138	17.92	3.511	14.29	1.363	0.507	0.2671
	IH	1.792	2.372	10.33	5.524	13.59	2.720	10.41	1.358	0.413	0.1899
FD NEQ Ko et al. (2020) (HKC18)	NH	2.400	1.860	12.46	7.080	27.56	5.361	22.62	1.349	0.343	0.335
	IH	1.640	5.270	8.382	7.804	27.83	5.318	22.94	1.353	0.671	0.410

D EQ (KCK19) NH result

The Astrophysical Journal, 937:116 (37pp), 2022 October 1 https://doi.org/10.3847/1538-4357/ac88cd

Comprehensive Analysis of the Neutrino Process in Core-collapsing Supernovae

Heamin Ko[1], Dukjae Jang[2], Myung-Ki Cheoun[1,3,4], Motohiko Kusakabe[3,4], Hirokazu Sasaki[4,5,6], Xingqun Yao[3], Toshitaka Kajino[3,4,5], Takehito Hayakawa[7,8], Masaomi Ono[9], Toshihiko Kawano[6], and Grant J. Mathews[3,4,10]
[1] Department of Physics and OMEG Institute, Soongsil University, Seoul 07040, Republic of Korea; cheoun@ssu.ac.kr
[2] Center for Relativistic Laser Science, Institute for Basic Science (IBS), Gwangju 61005, Republic of Korea
[3] School of Physics and International Research Center for Big-Bang Cosmology and Element Genesis, Beihang University, Beijing 100083, People's Republic of China
[4] National Astronomical Observatory of Japan, Mitaka, Tokyo 181-8588, Japan
[5] Graduate School of Science, The University of Tokyo, Bunkyo-ku, Tokyo 113-0033, Japan
[6] Theoretical Division, Los Alamos National Laboratory, Los Alamos, NM 87545, USA
[7] National Institutes for Quantum and Radiological Science and Technology, 2-4 Shirakata, Tokai, Naka, Ibaraki 319-1106, Japan
[8] Institute of Laser Engineering, Osaka University, Suita, Osaka 565-0871, Japan
[9] Kyushu University, Hakozaki, Fukuoka 812-8581, Japan
[10] Department of Physics, Center for Astrophysics, University of Notre Dame, Notre Dame, IN 46556, USA
Received 2022 April 24; revised 2022 August 5; accepted 2022 August 9; published 2022 October 4

Mass Fraction ratio of 7Li/11B and PF ration of 138La/11B

- The yield ratio of [7Li/11B]

$^{7}Li/^{11}B = -0.31 \pm 0.42$ **<0.53 (2 sigma)**

Spectra	FD	+SI	FD	+SI
Mass Hierarchy	IH	IH	NH	NH
Yield Ratio	0.671(0.488)	0.413(0.435)	0.343(0.342)	0.507(0.467)

The Astrophysical Journal Letters, 891:L24 (6pp), 2020 March 1 https://doi.org/10.3847/2041-8213/ab775b

Neutrino Process in Core-collapse Supernovae with Neutrino Self-interaction and MSW Effects

Heamin Ko[1], Myung-Ki Cheoun[1], Eunja Ha[1], Motohiko Kusakabe[2], Takehito Hayakawa[3], Hirokazu Sasaki[4], Toshitaka Kajino[2,4], Masa-aki Hashimoto[5], Masaomi Ono[6], Mark D. Usang[7], Satoshi Chiba[7], Ko Nakamura[8], Alexey Tolstov[9], Ken'ichi Nomoto[9], Toshihiko Kawano[10], and Grant J. Mathews[11]

- The production factor ratio of [138La/11B]

> 0.41 (lower limit)

$\mathrm{PF}[\mathrm{A}] = X_A / X_{A\odot}$ with X_A the mass fraction of A

Spectra	FD	+SI	FD	+SI
Mass Hierarchy	IH	IH	NH	NH
PF ratio	0.410(0.6585)	0.1899(0.3672)	0.335(0.6274)	0.2671(0.4776)

Contents

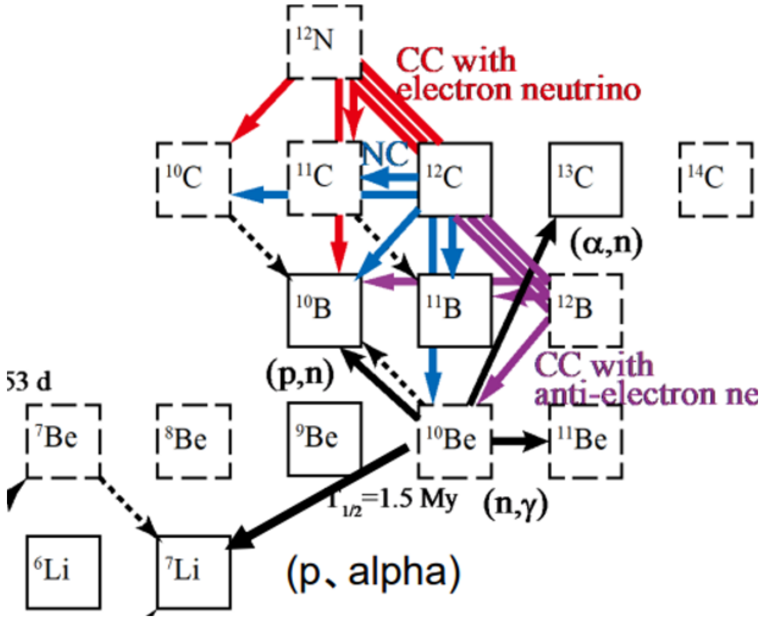

1. Motivation of the Neutrino-process

2. Cosmological Origin of ^{10}Be (Short-lived Radioactive Nucleus)

2-1. Ratio of $^{10}Be/^{9}Be$ by the Neutrino-process

2-2. Relevant Nuclear Reactions for ^{10}Be Production

3. Summary and Conclusion

10Be/9Be Ratio

Nuclear Abundance Ratio in the neutrino-process

nature COMMUNICATIONS

ARTICLE

Received 14 Jan 2016 | Accepted 20 Oct 2016 | Published 22 Nov 2016 DOI: 10.1038/ncomms13639 OPEN

Evidence from stable isotopes and ^{10}Be for solar system formation triggered by a low-mass supernova

Projjwal Banerjee[1], Yong-Zhong Qian[1], Alexander Heger[2,3] & W.C. Haxton[4]

other mechanisms in the CCSN. Mo
a given SLR, I its stable reference is
of R from the CCSN, and f the fr
incorporated into each $M_\odot$ of the
dilution factor). The number ratio o
this CCSN is

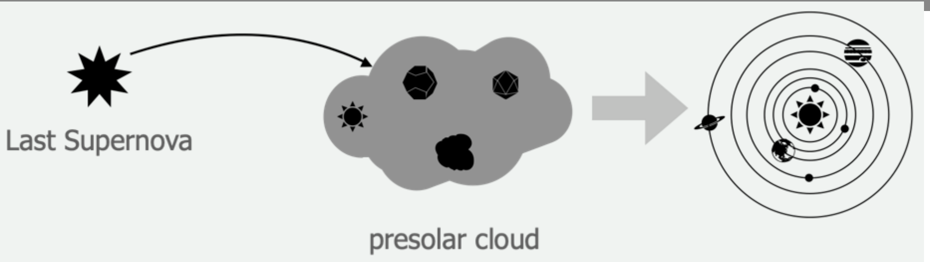

$$\left(\frac{N_R}{N_I}\right)_{\rm ESS} \sim \frac{f\,Y_R/A_R}{X_I^{\odot} M_\odot/A_I} \exp\left(-\frac{\Delta}{\tau_R}\right), \qquad (1)$$

where A_R and A_I are the mass numbers of R and I, $X_I^{\odot}$ is the solar mass fraction of I[30], Δ is the time between the CCSN explosion and incorporation of R into early SS solids, and τ_R is the lifetime of R.

Table 1 | Yields of short-lived radionuclides from an 11.8-solar-mass core-collapse supernova.

R/I	τ_R (Myr)	Y_R ($M_\odot$)	$X_I^{\odot}$	$(N_R/N_I)_{\rm ESS}$ Data	Case 1	Case 2	Case 3
^{10}Be/^{9}Be	2.00	3.26(−10)	1.40(−10)	(7.5 ± 2.5)(−4)	6.35(−4)	6.35(−4)	5.20(−4)
^{26}Al/^{27}Al	1.03	2.91(−6)	5.65(−5)	(5.23 ± 0.13)(−5)	1.02(−5)	9.90(−6)	5.77(−6)
^{36}Cl/^{35}Cl	0.434	1.44(−7)	3.50(−6)	∼(3-20)(−6)	2.00(−6)	1.45(−6)	6.15(−7)
^{41}Ca/^{40}Ca	0.147	3.66(−7)	5.88(−5)	(4.1 ± 2.0)(−9)	3.40(−9)	2.74(−9)	2.26(−9)
^{53}Mn/^{55}Mn	5.40	1.22(−5)	1.29(−5)	(6.28 ± 0.66)(−6)	4.04(−4)	6.39(−6)	6.16(−6)
^{60}Fe/^{56}Fe	3.78	3.08(−6)	1.12(−3)	∼1(−8);(5-10)(−7)	9.80(−7)	9.80(−7)	1.10(−7)
^{107}Pd/^{108}Pd	9.38	1.37(−10)	9.92(−10)	(5.9 ± 2.2)(−5)	6.27(−5)	6.27(−5)	5.72(−5)
^{135}Cs/^{133}Cs	3.32	2.56(−10)	1.24(−9)	∼5(−4)	7.51(−5)	7.51(−5)	3.18(−5)
^{182}Hf/^{180}Hf	12.84	4.04(−11)	2.52(−10)	(9.72 ± 0.44)(−5)	7.36(−5)	7.36(−5)	6.34(−6)
		8.84(−12)			1.60(−5)	1.60(−5)	2.37(−6)
^{205}Pb/^{204}Pb	24.96	9.20(−11)	3.47(−10)	∼1(−4);1(−3)	1.27(−4)	1.27(−4)	7.78(−5)

Comparisons are made to the corresponding isotopic ratios deduced from meteoritic data. Case 1 estimates are calculated from equation (1) using the approximate best-fit f and Δ of Fig. 2, assuming no fallback. The higher and lower yields for ^{182}Hf are obtained from the laboratory and estimated stellar decay rates[47] of ^{181}Hf, respectively. Case 2 (3) is a fallback scenario in which only 1.5% of the innermost 1.02 × 10^{-2} solar mass (0.116 solar mass) of shocked material is ejected. With guidance from refs 22,31, well-determined data are quoted with 2σ errors, while data with large uncertainties are preceded by '∼'. Note that $x(-y)$ denotes $x \times 10^{-y}$. Data references are: ^{10}Be (refs 14,16,18,19), ^{26}Al (refs 2,32), ^{36}Cl (refs 33-35), ^{41}Ca (refs 36,37), ^{53}Mn (ref. 38), ^{60}Fe (refs 39,40), ^{107}Pd (ref. 41), ^{135}Cs (ref. 42), ^{182}Hf (ref. 43) and ^{205}Pb (refs 44,45).

Nuclear Abundance Ratio in the neutrino-process

- Short-lived Radioactive Nuclei

Progress in Particle and Nuclear Physics, (2018), 1-47, 102

Table 3
List of stellar nucleosynthesis sites and the nucleosynthetic processes occurring within them that are responsible for the production of th
reference isotopes listed in Column 3. Column 4 indicates if the site of production is important in terms of GCE (**M**=Major) or not (*m*=mino
that it is still debated whether the site is major or minor. Indicative references are listed in Column 5.

Stellar site	Process	Products	Relevance	
Low-mass AGBs	*s* process	^{107}Pd, ^{108}Pd	M	
		^{135}Cs, ^{133}Cs	M	
		^{182}Hf, ^{180}Hf	M	
		^{205}Pb, ^{204}Pb	M	
Massive and Super-AGBs	p captures	^{26}Al	*m*	
	n captures	^{41}Ca, ^{36}Cl, ^{60}Fe	*m*	
	s process	^{107}Pd, ^{135}Cs, ^{182}Hf	*m*	
WR stars	p captures	^{26}Al	M	
	n captures	^{41}Ca, ^{36}Cl	*m*	
	n captures	^{97}Tc, ^{107}Pd, ^{135}Cs, ^{205}Pb	*m*	
CCSNe	p captures+explosive	^{26}Al, ^{27}Al	M	
	n captures	^{60}Fe	M	
	n captures	^{36}Cl, ^{41}Ca	M	
	C/Ne/O burning	^{35}Cl, ^{40}Ca	M	
	NSE	^{53}Mn, ^{55}Mn, ^{56}Fe	M/*m*[a]	
	n captures	^{107}Pd, ^{126}Sn, ^{135}Cs	*m*	
		^{129}I, ^{182}Hf, ^{205}Pb	*m*	
	α-rich freezeout	^{92}Nb, ^{92}Mo, ^{97}Tc, ^{98}Tc	M/*m*	[103]
	γ process	^{144}Sm, ^{146}Sm	M/*m*	[103,104]
	ν process	^{10}Be, ^{92}Nb	*m*	[105,106]
SNIa	NSE	^{53}Mn, ^{55}Mn, ^{56}Fe	M	[107]
	γ process	^{92}Nb, ^{93}Nb, ^{146}Sm, ^{144}Sm	M/*m*	[108]
		^{97}Tc, ^{98}Tc, ^{98}Ru	M/*m*	
NSMs/special CCSNe	*r* process	^{107}Pd, ^{108}Pd, ^{126}Sn, ^{124}Sn	M	[109][b]
		^{135}Cs, ^{133}Cs, ^{129}I, ^{127}I	M	
		^{182}Hf, ^{180}Hf	M	
		^{247}Cm, ^{235}U, ^{244}Pu, ^{238}U	M	[110,111]
novae	p captures	^{26}Al	*m*	[112]
CRs	non-thermal	^{7}Be, ^{10}Be, ^{9}Be	M	[32]
		^{26}Al, ^{41}Ca, ^{36}Cl, ^{53}Mn	*m*	[113]

[a] The current understanding is that roughly 1/3 of the abundances of the Fe-peak elements in the Galaxy are produced by CCSNe, with the rest coming from SNIa.
[b] Abundances to be derived using the *s*-process predictions provided in the reference via the *r*-residual method, where the *r*-process abundance is given by the Solar System abundance minus the *s*-process abundance.

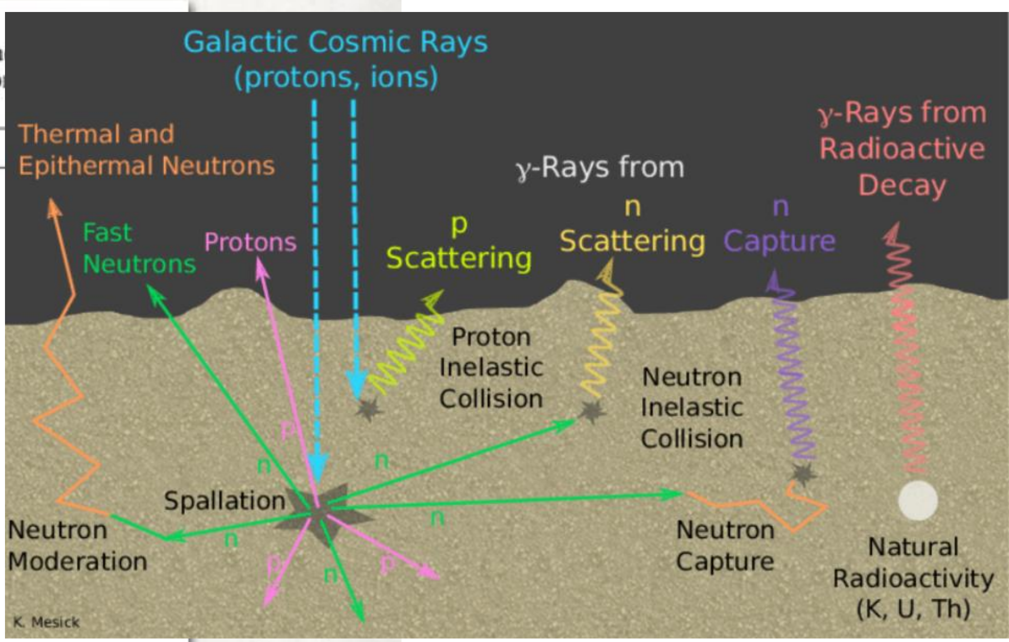

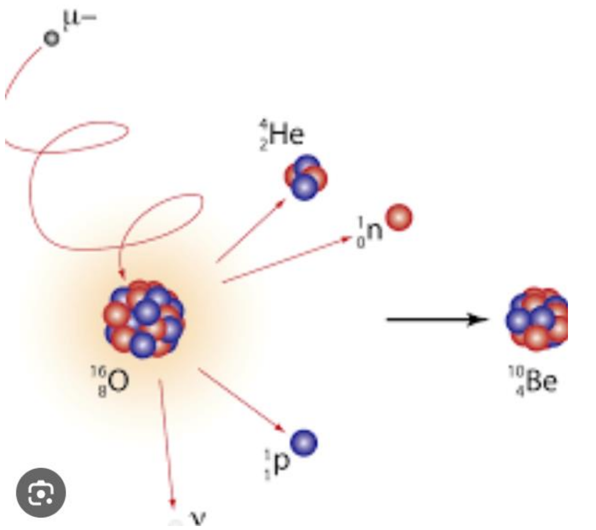

[105] Nature Communications, (2016), 7

Contents

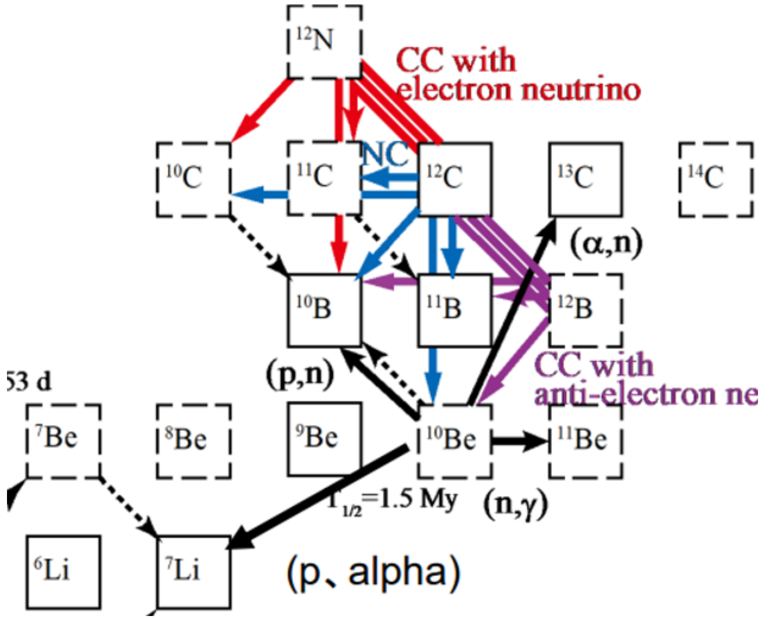

1. Motivation of the Neutrino-process

2. Cosmological Origin of ^{10}Be (Short-lived Radioactive Nucleus)

2-1. Ratio of ^{10}Be/^{9}Be by the Neutrino-process

2-2. Relevant Nuclear Reactions for ^{10}Be Production

3. Summary and Conclusion

$^{16}O(nu,...)^{10}Be$ & $^{12}C(nu,...)^{10}Be$

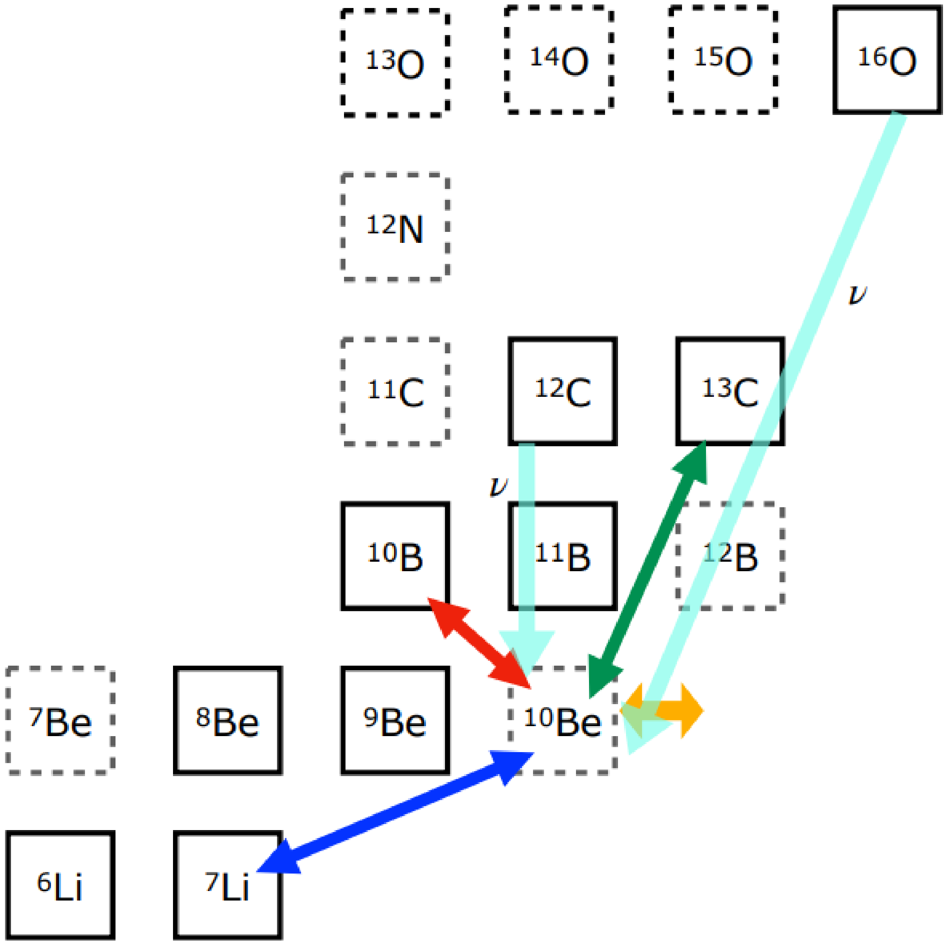

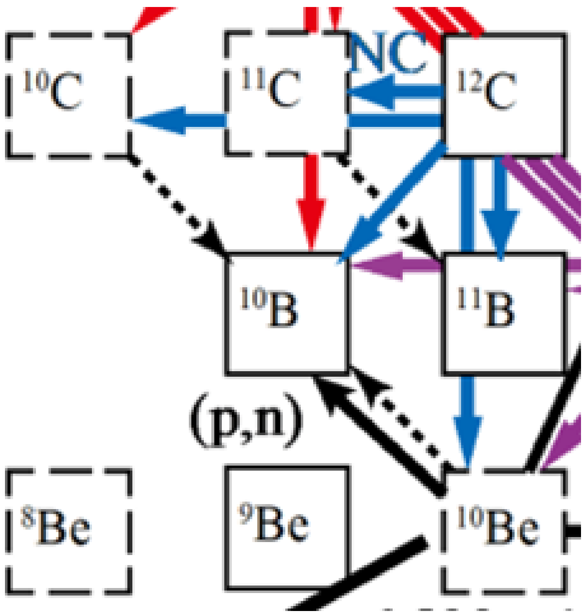

Two step process !!

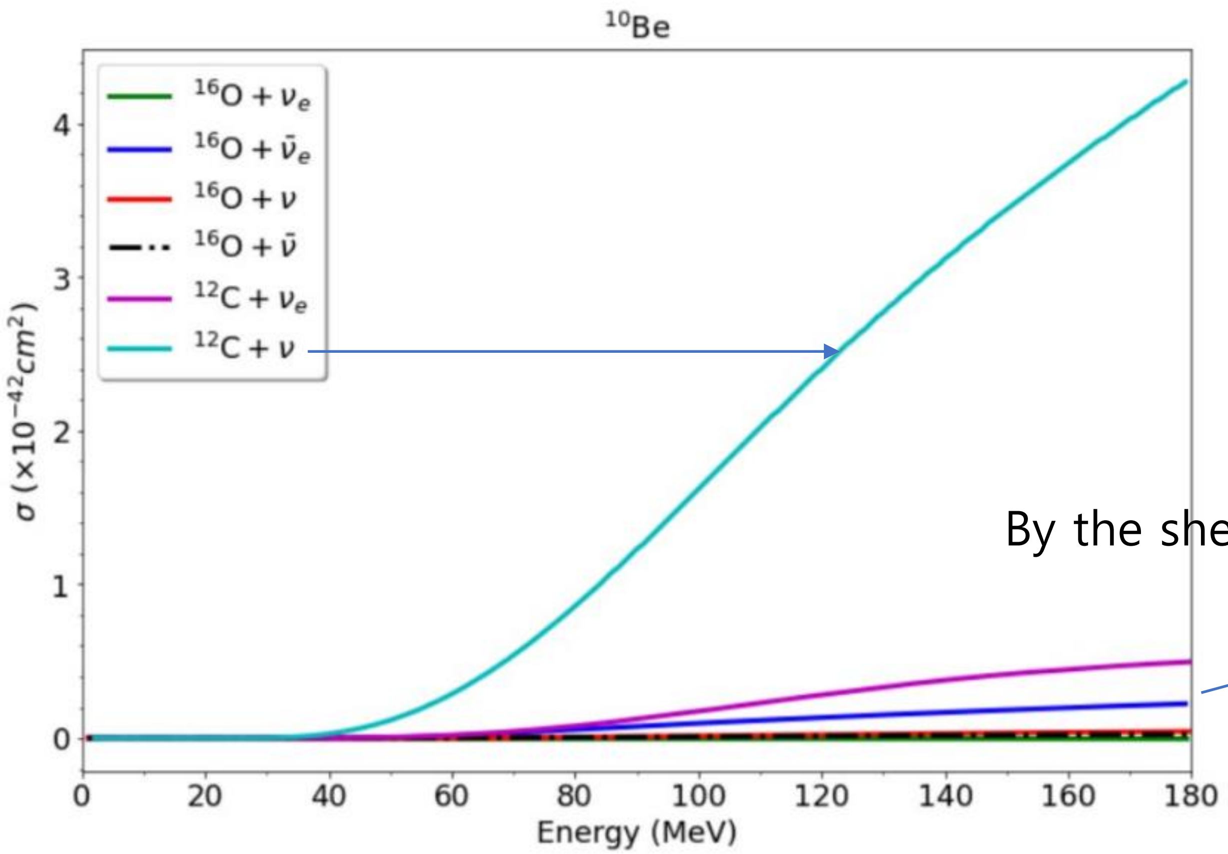

FIG. 2: (Color online) Comparisons of neutrino induced reactions on ^{12}C and ^{16}O calculated from the shell model [4]. These include all of the particle emitting decay channels from the compound nuclei produced by CC and NC neutrino reactions.

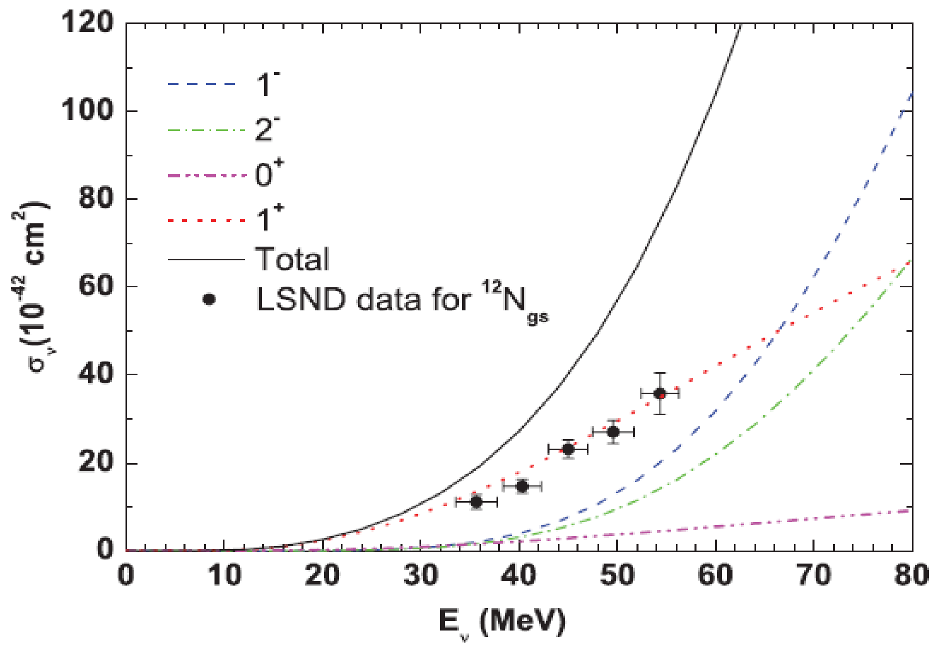

By the shell model

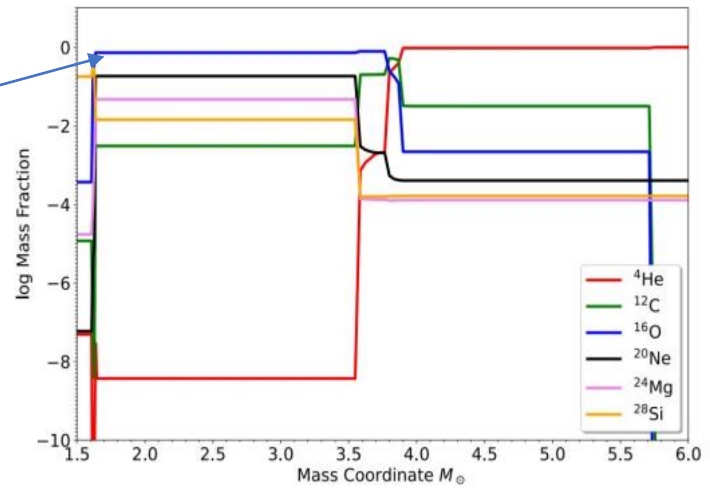

FIG. 7: (Color online) Mass fractions of pre-supernova. $M_\odot \leq 3.5$ region is O-Ne-Mg region followed by He-C-O region.

$^{10}Be\ (p,n)^{10}B$ & $^{10}B\ (n,p)^{10}Be$

$$Q_{^{10}Be(p,n)^{10}B} = -0.225499\ \text{MeV}$$

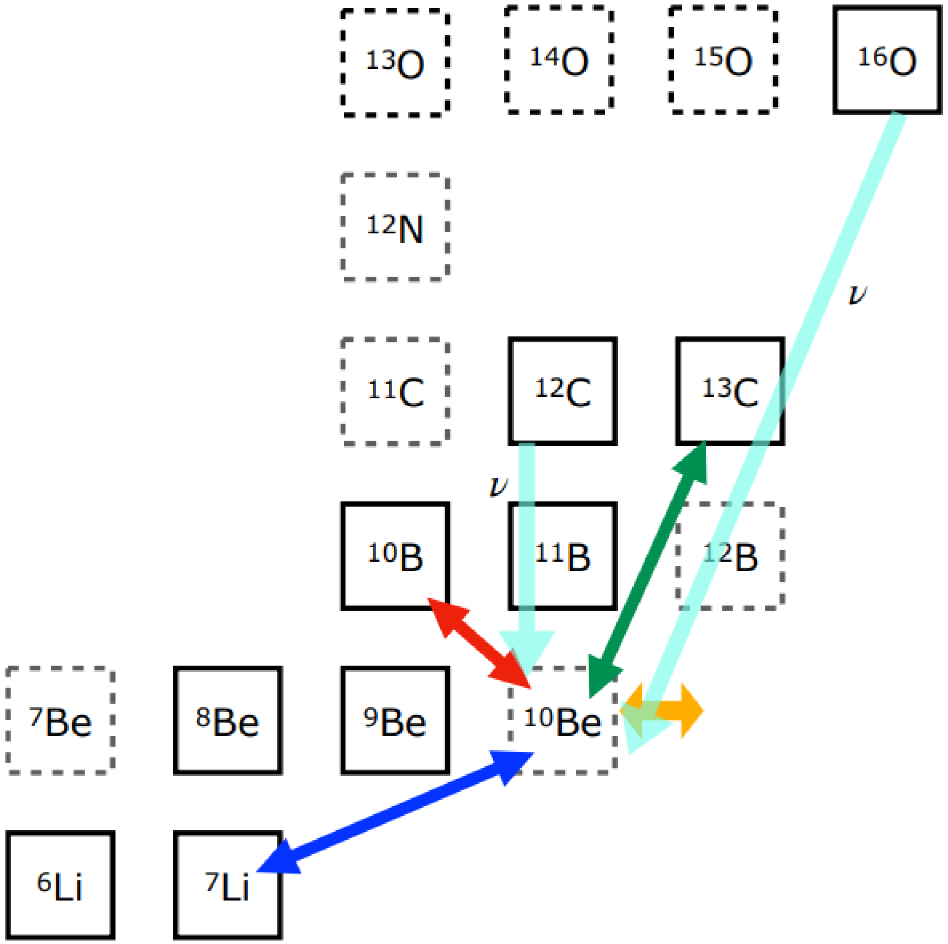

JENDL-4.0

- 스크린샷 $^{10}B(n,p)^{10}Be$

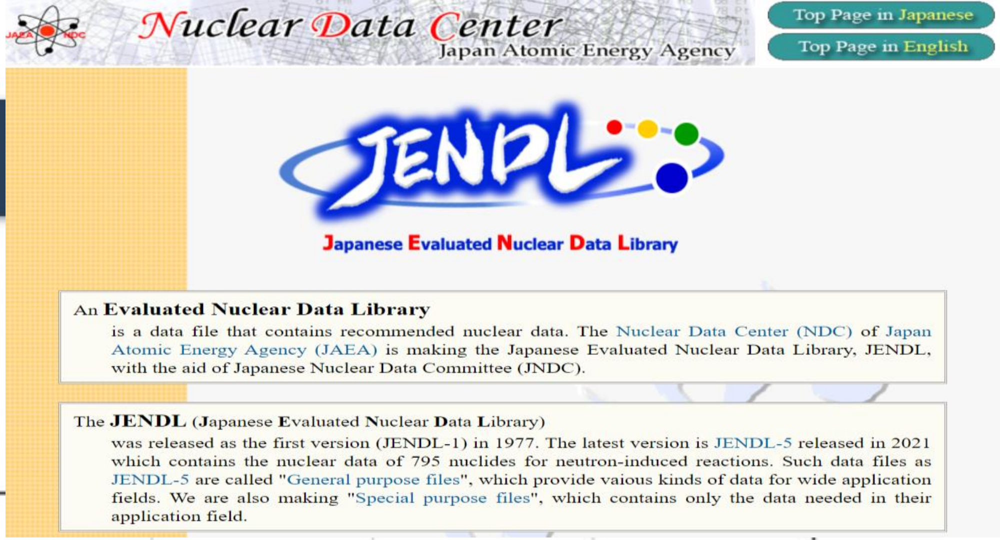

Nuclear Data Center
Japan Atomic Energy Agency
Top Page in Japanese
Top Page in English

JENDL
Japanese Evaluated Nuclear Data Library

An Evaluated Nuclear Data Library
is a data file that contains recommended nuclear data. The Nuclear Data Center (NDC) of Japan Atomic Energy Agency (JAEA) is making the Japanese Evaluated Nuclear Data Library, JENDL, with the aid of Japanese Nuclear Data Committee (JNDC).

The **JENDL** (**J**apanese **E**valuated **N**uclear **D**ata **L**ibrary)
was released as the first version (JENDL-1) in 1977. The latest version is JENDL-5 released in 2021 which contains the nuclear data of 795 nuclides for neutron-induced reactions. Such data files as JENDL-5 are called "General purpose files", which provide vaious kinds of data for wide application fields. We are also making "Special purpose files", which contains only the data needed in their application field.

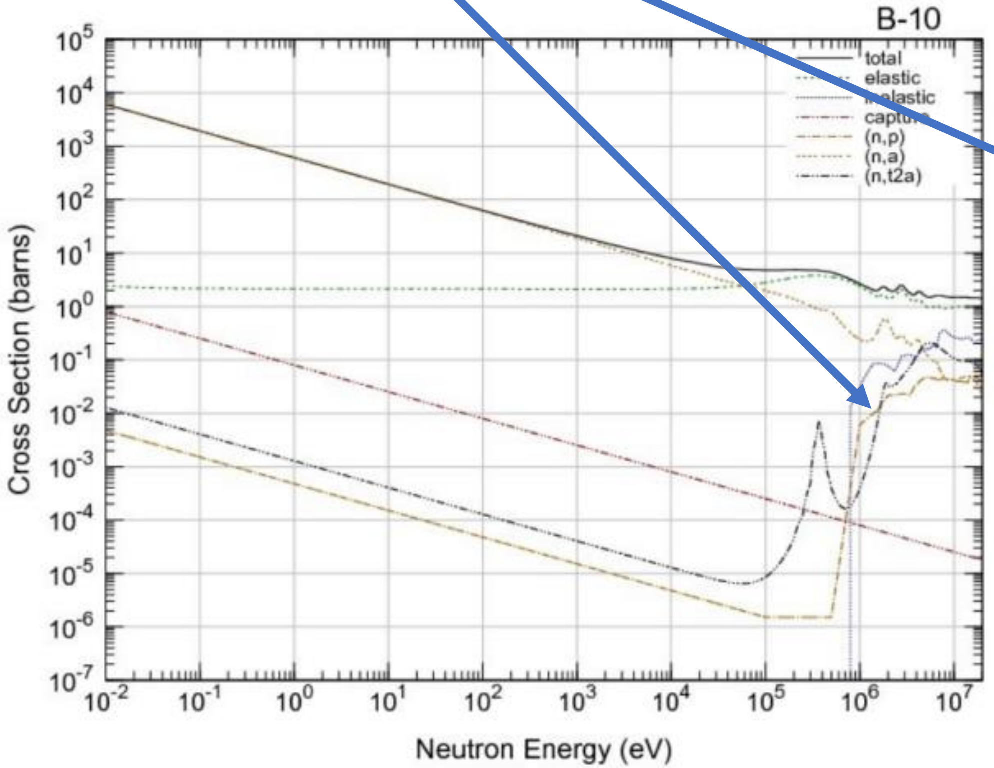

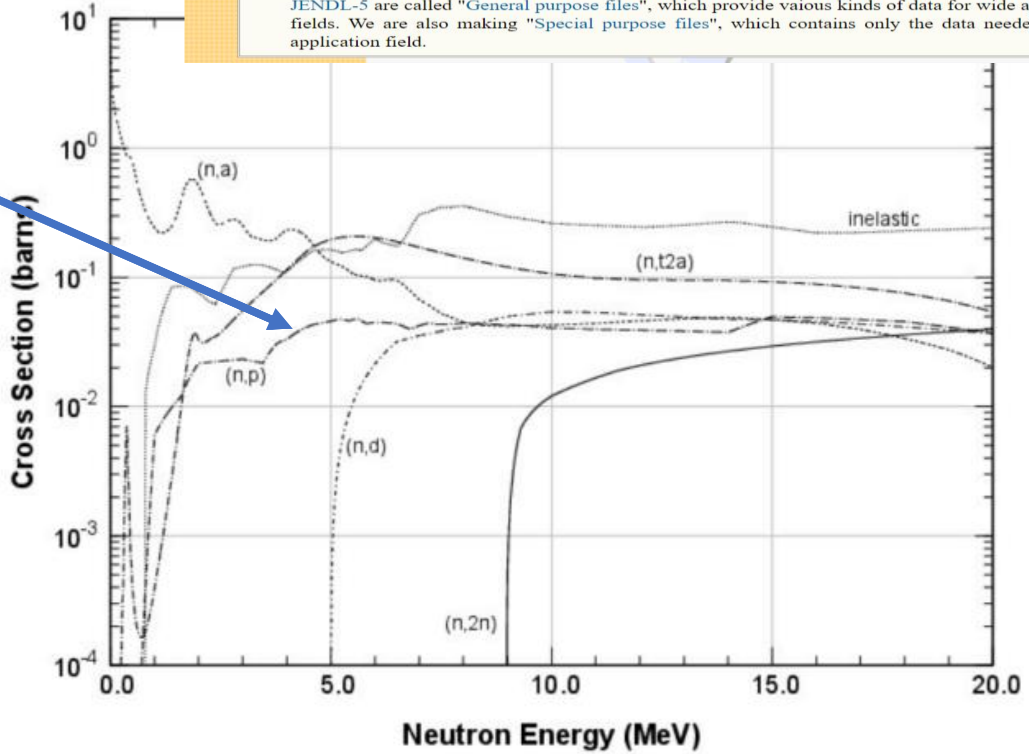

Analysis of each case

- 1.3 ^{10}Be(p,n)^{10}B data **comparison**

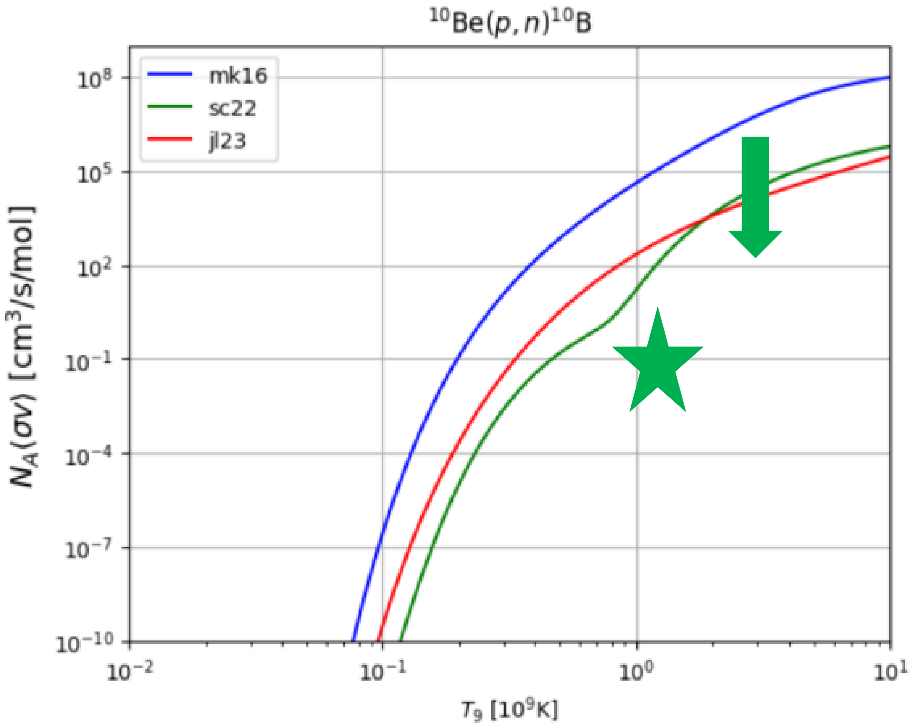

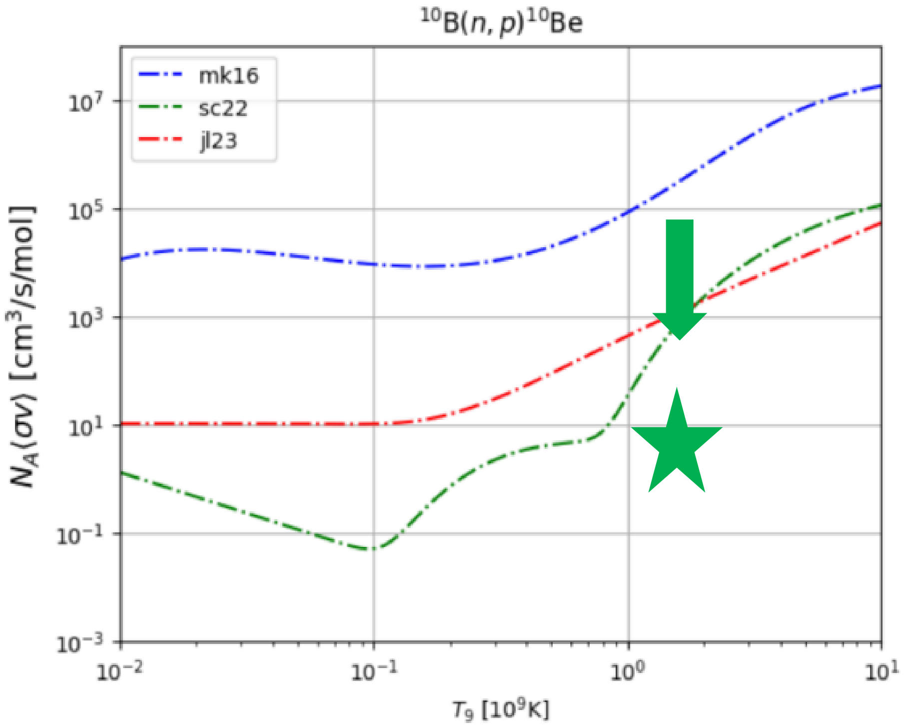

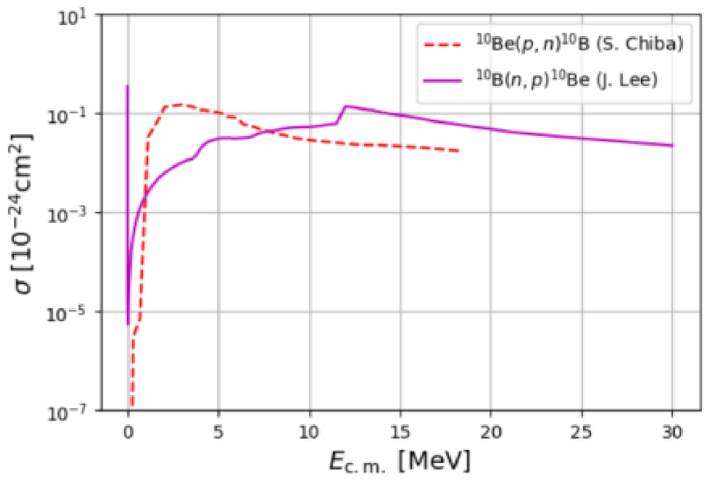

raw cross section data

1. ^{10}Be$(p,n)^{10}$B Q-value = -0.22559 MeV
   - mk16 - TALYS-1.8 code (2015)
   - sc22 - S. Chiba (g.s. from JENDL-5)
   - jl23 - J. Lee

$^{10}Be(p,\alpha)^{7}Li$ (Q-value = 2.56411 MeV)

$^{10}Be\ (p,a)^{7}Li\ \&\ ^{7}Li\ (a,p)^{10}Be$

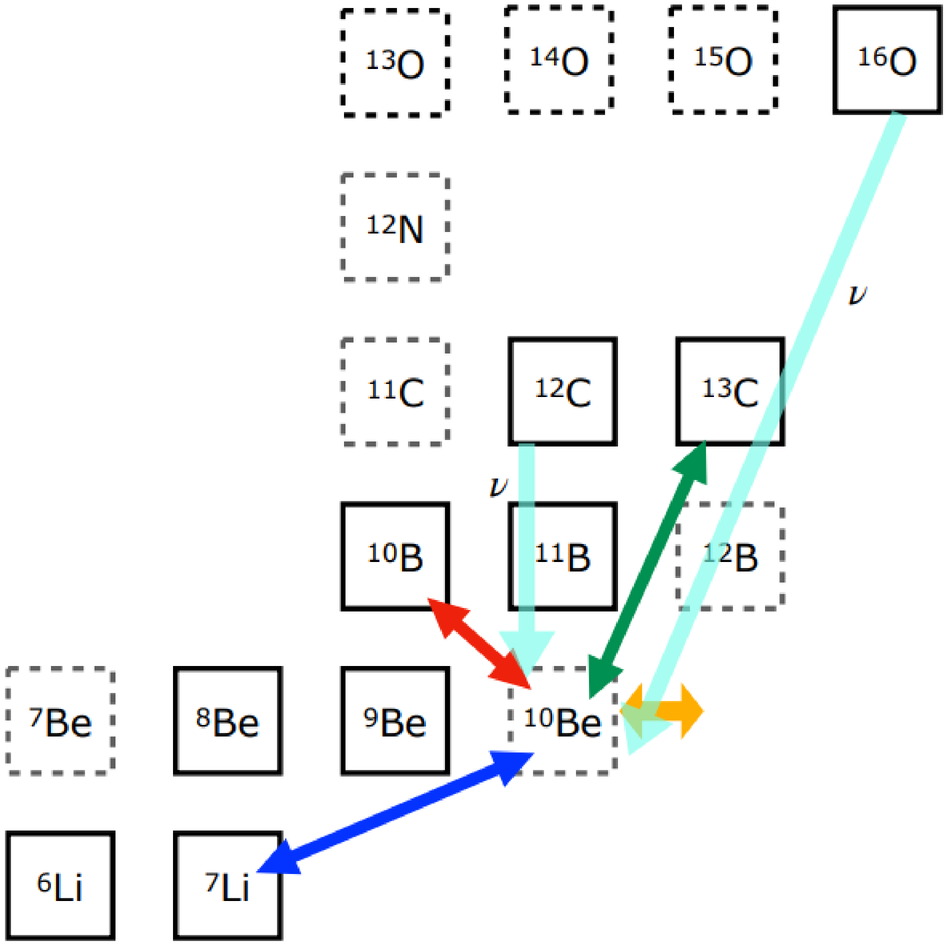

Role of low-lying resonances for the ^{10}Be$(p,\alpha)^7$Li reaction rate and implications for the formation of the Solar System

A. Sieverding,[1,*] J. S. Randhawa,[2] D. Zetterberg,[1,3] R. J. deBoer,[2] T. Ahn,[2] R. Mancino,[4,5] G. Martínez-Pinedo,[5,4] and W. R. Hix[1,3]

Energy (MeV)	J^π	partial widths (keV)
11.272	$9/2^+$	$\Gamma_p = 10^{-15}, \Gamma_\alpha = 110$
11.425	$1/2^+$	$\Gamma_p = 6, 11, \Gamma_\alpha = 6, 1$
11.490	$3/2^+$	$\Gamma_p = 10^{-4}\ \Gamma_\alpha = 93$
11.600	$5/2^+$	$\Gamma_p = 10^{-5}, \Gamma_\alpha = 90, \Gamma_n = 90$
11.893	$5/2^-$	$\Gamma_p = 10^{-4}, \Gamma_\alpha = 100, \Gamma_n = 94$
12.040	$7/2^+$	$\Gamma_p = 10^{-3}, \Gamma_\alpha = 500, \Gamma_n = 500$
12.550	$1/2^+$	$\Gamma_p = 100, \Gamma_\alpha = 105$

they can explain the puzzling β^-p$^+$ decay in ^{11}Be. A recent experiment, which directly measured the protons and their energy distribution, shows that the decay proceeds sequentially though a narrow resonance [$E = 11425(20)$ keV, $\Gamma = 12(5)$ keV, $J^\pi = (1/2^+, 3/2^+)$] in ^{11}B [44]. Preceeding this experiment, it was shown that shell model embedded in the continuum (SMEC) calculations strongly favor the $J^\pi = 1/2^+$ assignment over $3/2^+$ [45]. This $1/2^+$ resonance at $\approx$193 keV[^{11}B $S(p) = 11228$ keV], proves to be most crucial for the ^{10}Be$(p,\alpha)^7$Li reaction rate as it is well within the Gamow window and provides the dominant contribution to ^{10}Be$(p,\alpha)^7$Li reaction rate throughout, as discussed in detail below.

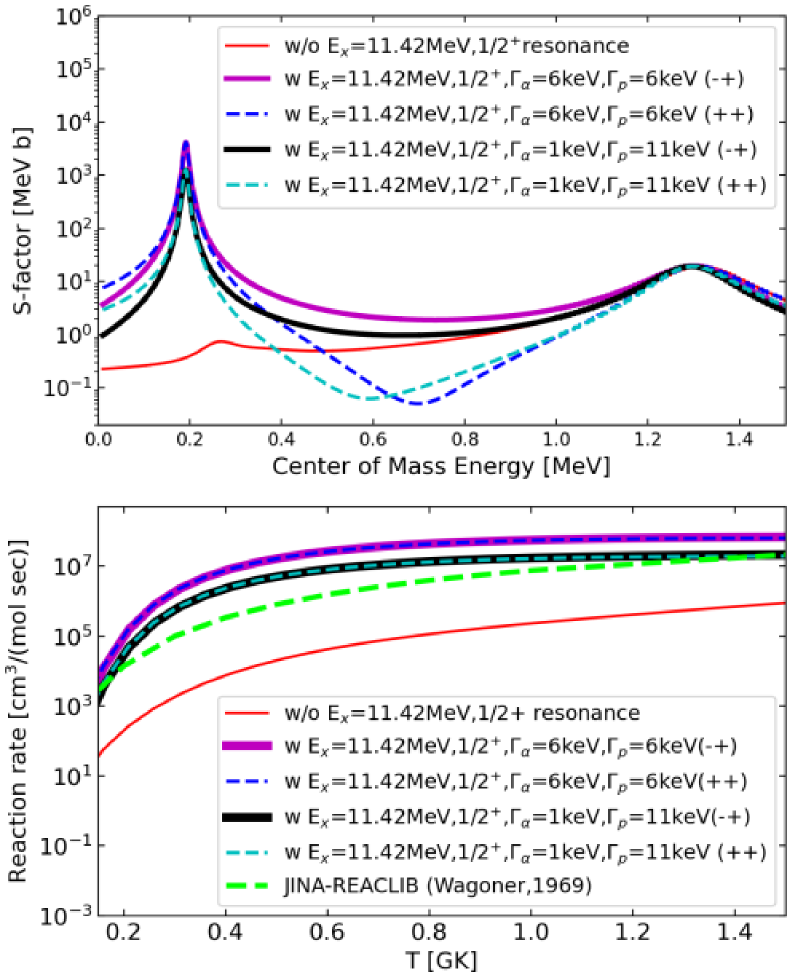

FIG. 6. *R*-matrix calculations to assess the impact of the 193 keV $1/2^+$ resonance on the ^{10}Be(p,α) reaction cross section. The top panel shows the S factor and the bottom panel the reaction rate as a function of temperature. Results without the 193 keV $1/2^+$ resonance are shown (red line) as well as several results assuming different resonance widths and assumptions about the interference with the $3/2^+$ resonance (see text). For comparison, the rate from Ref. [22] is also shown (green dashed line). The result with $\Gamma_p = 6$ keV, $\Gamma_\alpha = 6$ keV, $(+-)$ is the new recommended rate.

Analysis of each case

^{10}Be(p,a)^{7}Li data **comparison**

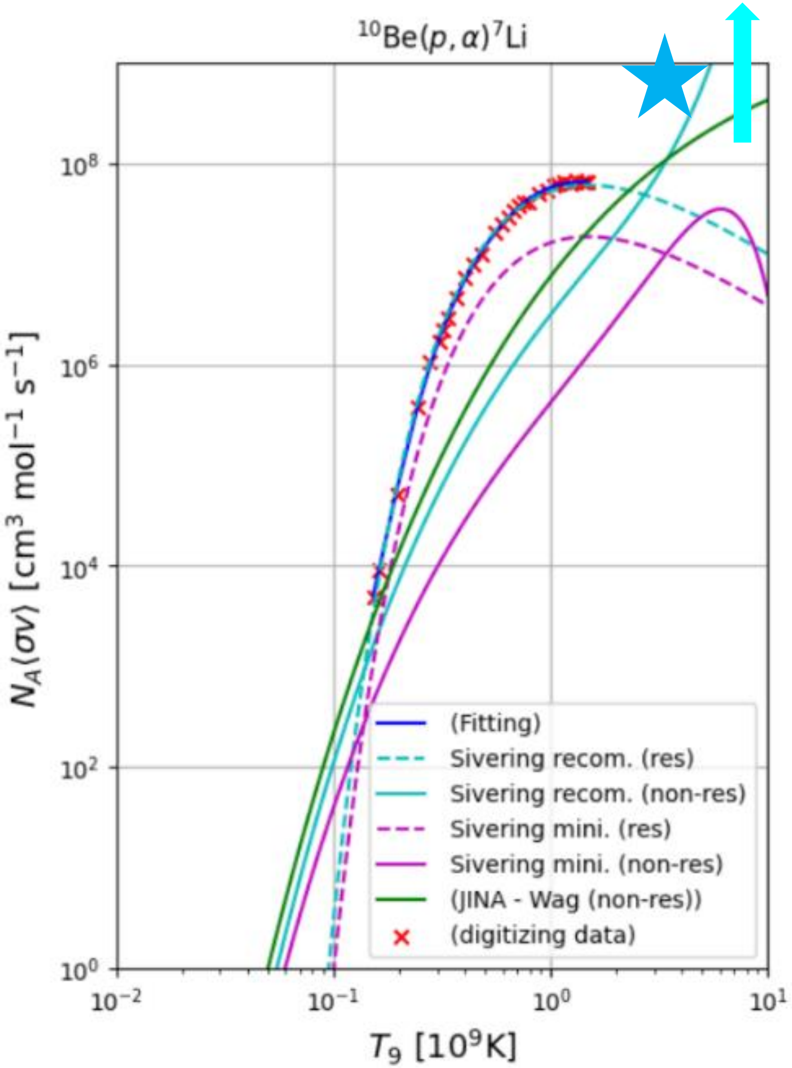

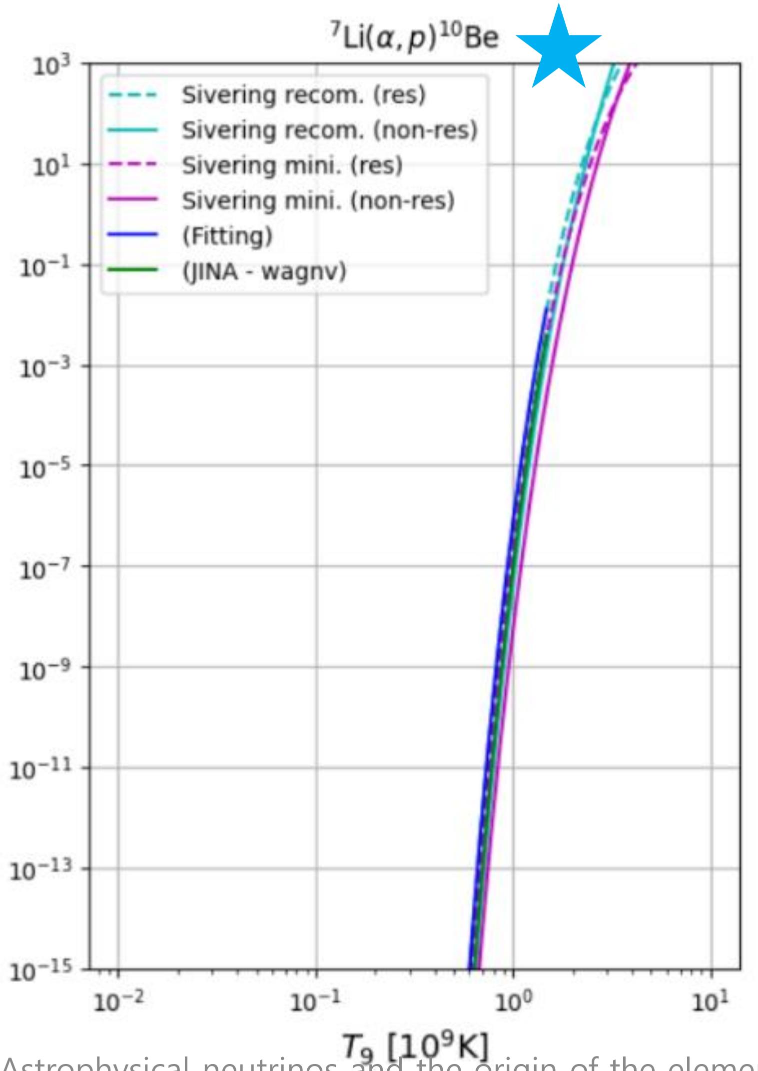

TABLE IV. Fit parameters for the minimum and recommended rate. Each rate consists of a resonant and non-resonant contribution.

	Minimum		Recommended	
	resonant	non-resonant	resonant	non-resonant
a_0	18.83813	30.49055	20.01675	29.05572
a_1	-2.236187	0.0	-2.236187	0.0
a_2	0.0	-11.32177	0.0	-11.25624
a_3	0.0	-9.265300	0.0	-3.687460
a_4	0.0	3.559158	0.0	0.7607396
a_5	0.0	-0.5154761	0.0	0.08781213
a_6	-1.5	-2/3	-1.5	-2/3

A. Sieverding et al. Phys. Rev.C 106, 015803 (2022)

We adopt the recommended resonant reaction rate parameters. (cyan color dashed-line)

Q value is 3.83555 MeV

^{10}Be (a,n)^{13}C & ^{13}C (n,a)^{10}Be

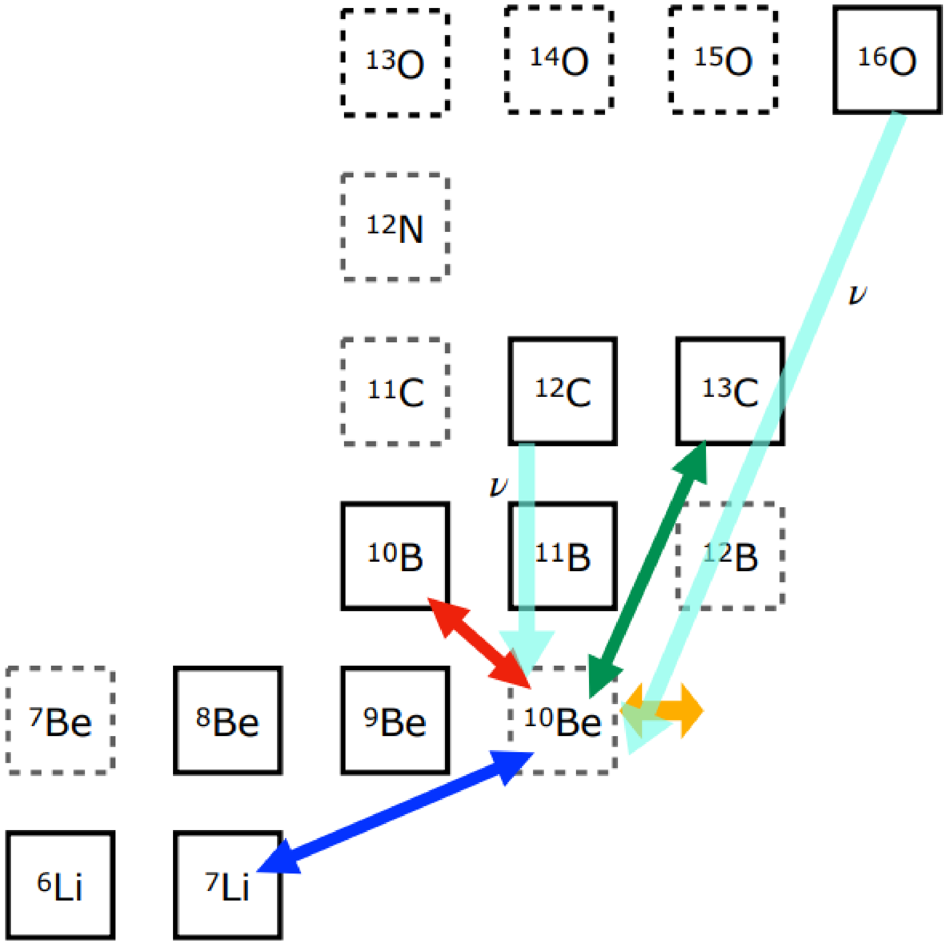

Analysis of each case

$^{13}C\ (n,a)^{10}Be$ data **JENDL-5**

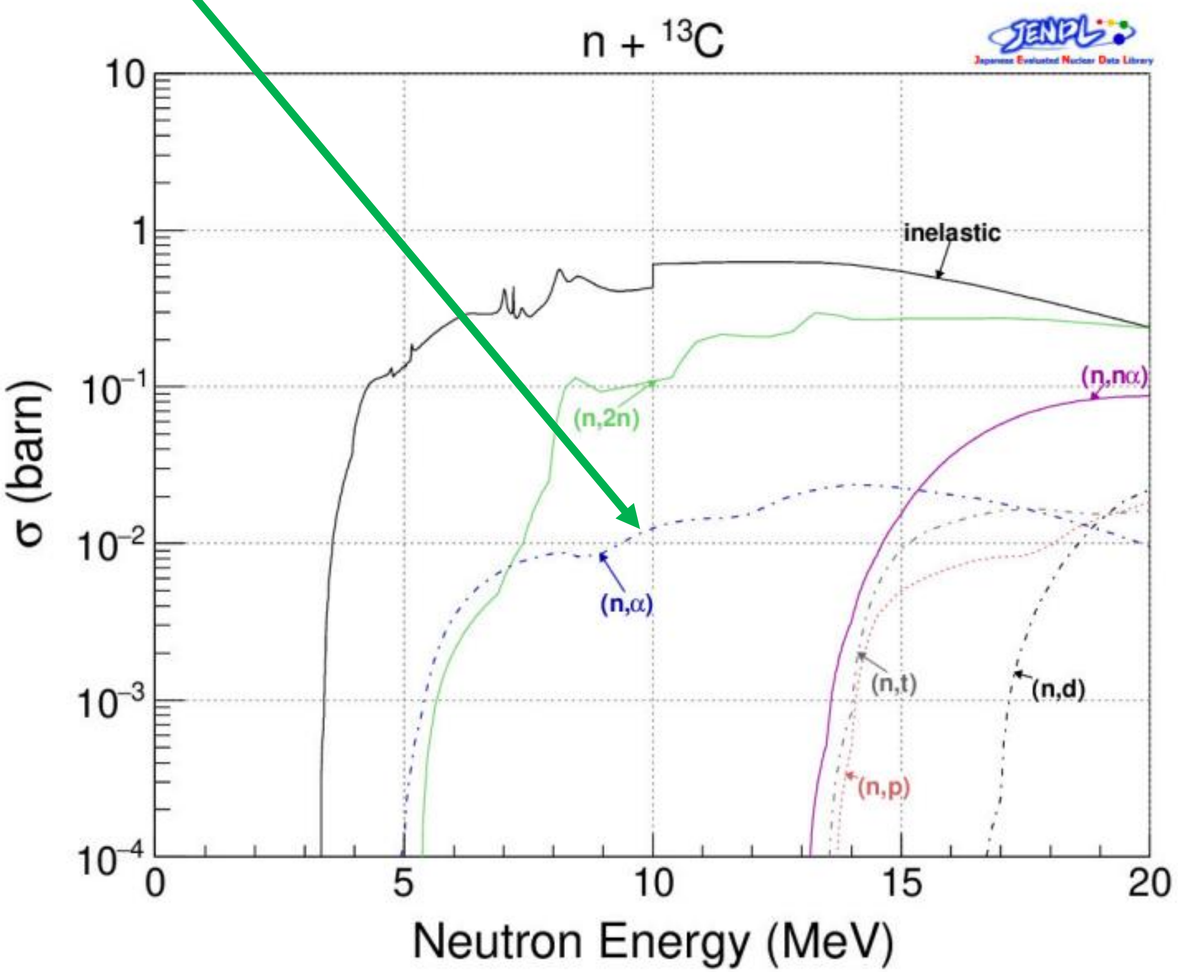

Maxwellian Average :

$$\sigma_{macs}(T) = \frac{2}{\sqrt{\pi}} \frac{\int_{E_L}^{E_U} \sigma(E,T) \cdot E \cdot \exp\left(-\frac{E}{k_B T}\right) dE}{\int_{E_L}^{E_U} E \cdot \exp\left(-\frac{E}{k_B T}\right) dE},$$

where T denotes the temperature, and k_B the Boltzmann constant. The upper and lower limits of integration, E_L and E_U are set to 10^{-5} eV and 10 eV, respectively.

Resonance Integral :

$$\sigma_{ri}(T) = \int_{E_L}^{E_U} \sigma(E,T) \cdot \frac{1}{E}\, dE,$$

with $E_L = 0.5$ eV and $E_U = 10$ MeV.

U-235 Thermal Fission-Neutron Spectrum Average (Fiss. Spec. Average) :

$$\sigma_{facs}(T) = \frac{\int_{E_L}^{E_U} \sigma(E,T) \cdot \sqrt{\frac{4}{\pi a^3 b}} \cdot \exp\left(-\frac{ab}{4} - \frac{E}{a}\right) \cdot \sinh\sqrt{bE}\, dE}{\int_{E_L}^{E_U} \sqrt{\frac{4}{\pi a^3 b}} \cdot \exp\left(-\frac{ab}{4} - \frac{E}{a}\right) \cdot \sinh\sqrt{bE}\, dE},$$

with $E_L = 10^{-5}$ eV and $E_U = 20$ MeV. The parameters a and b are 0.988 MeV and 2.249 MeV^{-1}, respectively. The fission spectrum is based on Watt's formula (Phys. Rev. 87, 1041 (1952)).

Westcott g-factor :

$$g(T) = \frac{\sigma_{macs}(T)}{\sigma(0.0253\ \mathrm{eV}, T)}.$$

ν_p, ν_d : numbers of prompt and delayed neutrons per fission.

I got the data at https://www-nds.iaea.org/exfor/servlet/E4sGetTabSect?SectID=14385643&req=10221&PenSectID=19009181

Analysis of each case

- 3. $^{10}Be(a,n)^{13}C$ data **comparison**

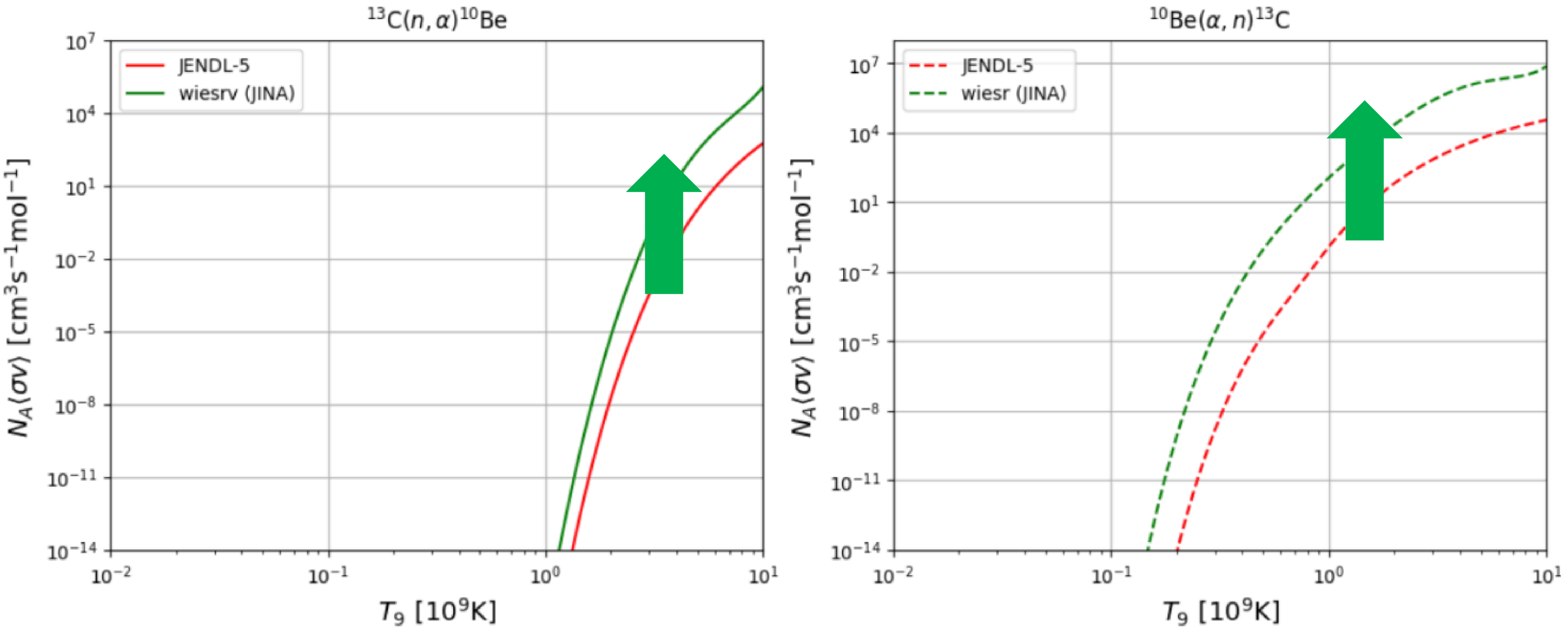

3. $^{10}Be(\alpha,n)^{13}C$ Q-value = 3.83555 MeV

- wiesr (JINA) - various refs. M. wiescher (2000)
  (r: resonate rate)
- jnd5 - JENDL-5 ($^{13}C(n,\alpha)^{10}Be$ reaction cross section)

$^{10}\mathrm{Be}(n,\gamma)^{11}\mathrm{Be}$ Q-value = 0.504369 MeV

^{11}Be (g,n)^{10}Be & ^{10}Be (n,g)^{11}Be

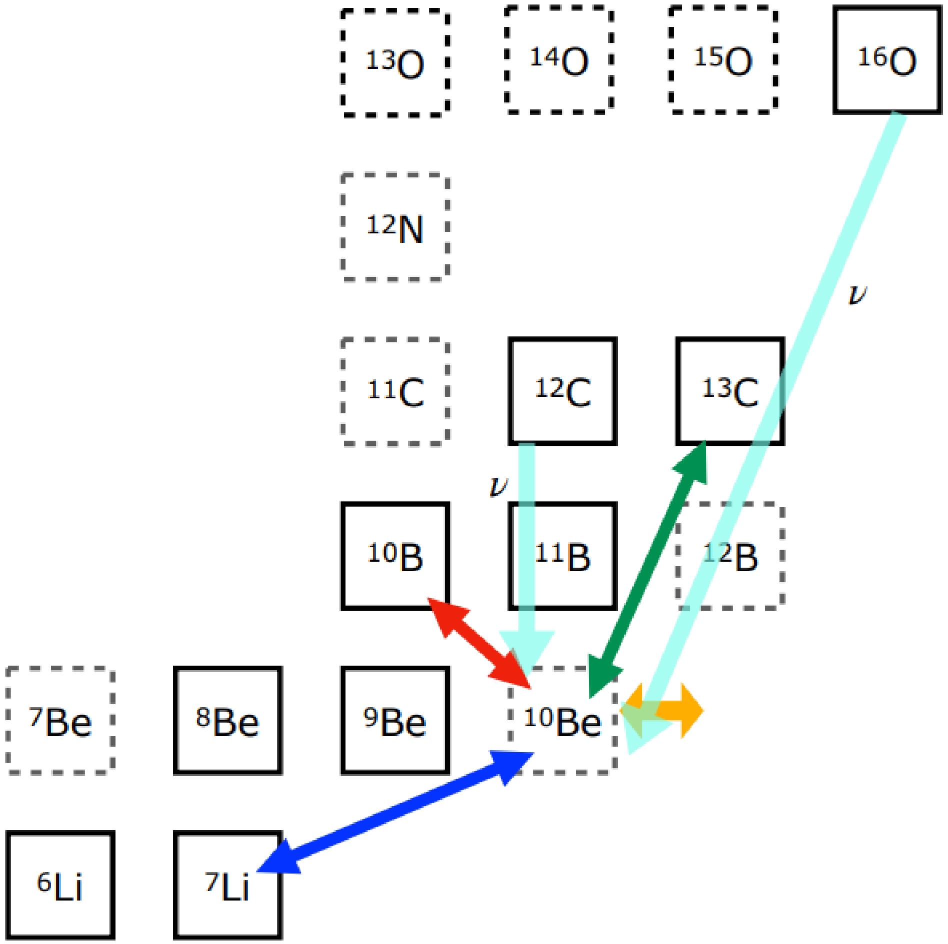

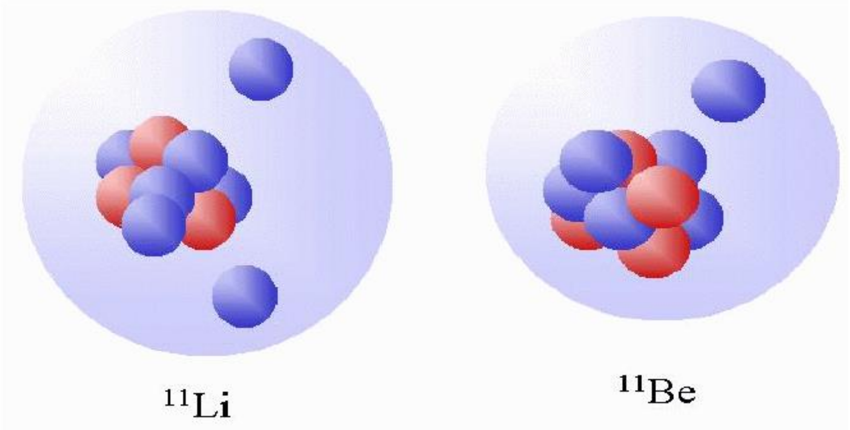

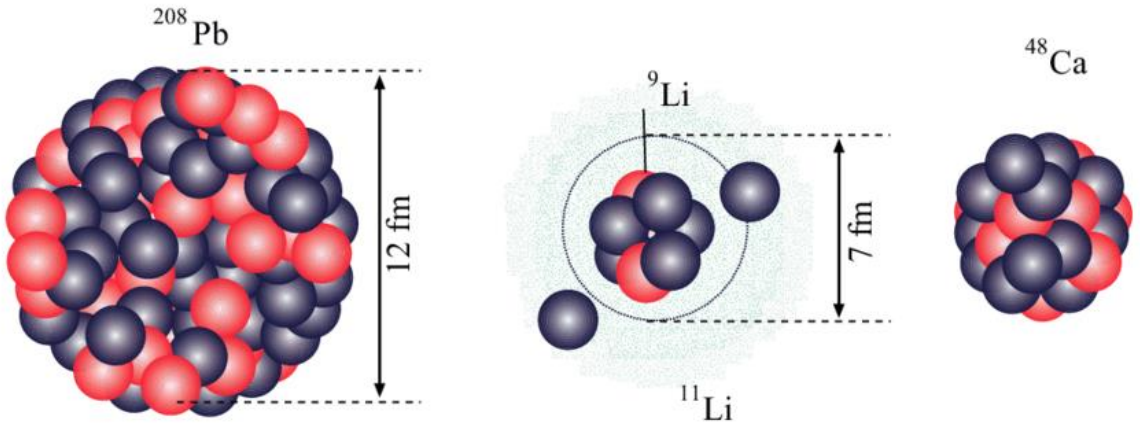

ELSEVIER

Physics Letters B 331 (1994) 296–301

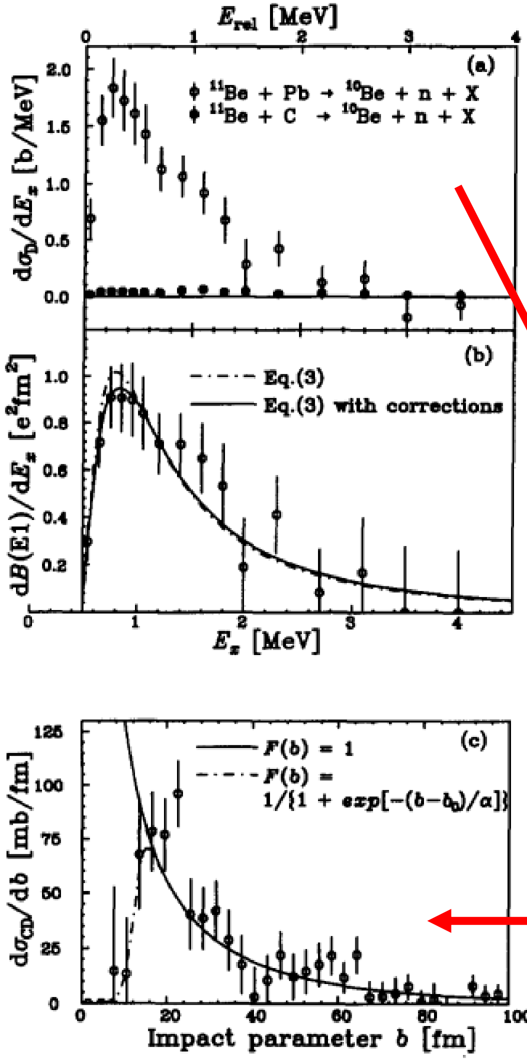

Fig. 1. (a) Dissociation cross sections of ^{11}Be on a Pb target as a function of the excitation energy E_x or relative energy E_{rel} for the ^{10}Be+n system. Data from a C target are also indicated. (b) Dipole strengths deduced from the $d\sigma_{CD}/dE_x$ spectrum are shown by the open circles. The dot-dashed line indicates the $dB(E1)/dE_x$ spectrum calculated using the direct breakup model (Eq. (3)). The solid line represents the associated theoretical distribution including the effects of detector resolution and Coulomb post acceleration. (c) Impact parameter dependence of the Coulomb dissociation cross section. The curves are theoretical (see text). The error bars in (a)–(c) are purely statistical.

Coulomb dissociation of a halo nucleus ^{11}Be at 72*A* MeV

T. Nakamura [a,1], S. Shimoura [a,2], T. Kobayashi [b], T. Teranishi [a], K. Abe [c], N. Aoi [a], Y. Doki [a], M. Fujimaki [b], N. Inabe [b], N. Iwasa [d], K. Katori [c], T. Kubo [b], H. Okuno [a], T. Suzuki [b], I. Tanihata [b], Y. Watanabe [b], A. Yoshida [b], M. Ishihara [a,b]

[a] *Department of Physics, University of Tokyo, 7-3-1 Hongo, Bunkyo, Tokyo 113, Japan*
[b] *The Institute of Physical and Chemical Research (RIKEN), 2-1 Hirosawa, Wako, Saitama 351-01, Japan*
[c] *Department of Physics, Osaka University, 1-1 Machikaneyama, Toyonaka, Osaka 560, Japan*
[d] *Department of Physics, Rikkyo University, 3 Nishi-Ikebukuro, Toshima, Tokyo 171, Japan*

Received 4 February 1994; revised manuscript received 18 April 1994
Editor: J.P. Schiffer

According to the equivalent photon method [17], $d\sigma_{CD}/dE_x$ is related to the dipole strength distribution $dB(E1)/dE_x$ as follows:

$$\frac{d\sigma_{CD}(E_x)}{dE_x} = \int_{b_0}^{\infty} 2\pi b db \frac{N_{E1}(E_x, b)}{E_x} \sigma_\gamma^{E1}(E_x) \qquad (1)$$

$$\frac{dB(E1)}{dE_x} = \frac{9\hbar c}{16\pi^3} \frac{\sigma_\gamma^{E1}(E_x)}{E_x}, \qquad (2)$$

where $N_{E1}(E_x, b)$ is the number of virtual photons with energy E_x in a collision at impact parameter b, while $\sigma_\gamma^{E1}(E_x)$ represents the E1 photo-absorption cross section at E_x. The cutoff impact parameter b_0 can be determined by observing the impact parameter dependence of the cross section as described later.

Coulomb Breakup

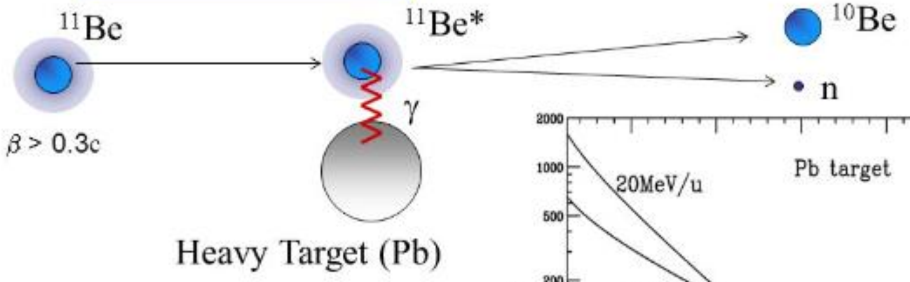

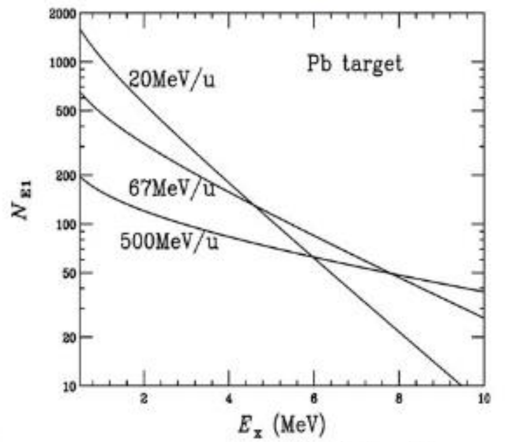

Excitation Energy
(=Photon Energy)

- Excitation by a Virtual Photon

$$\frac{d\sigma_C}{dE_x} = \frac{16\pi^3}{9\hbar c} N_{E1}(E_x) \frac{dB(E1)}{dE_x}$$

Cross Section = (Photon Number) x (Transition Probability)

- Invariant Mass Spectroscopy

Analysis of each case

- 4.2 $^{11}Be(\gamma,n)^{10}Be$ data **comparison**

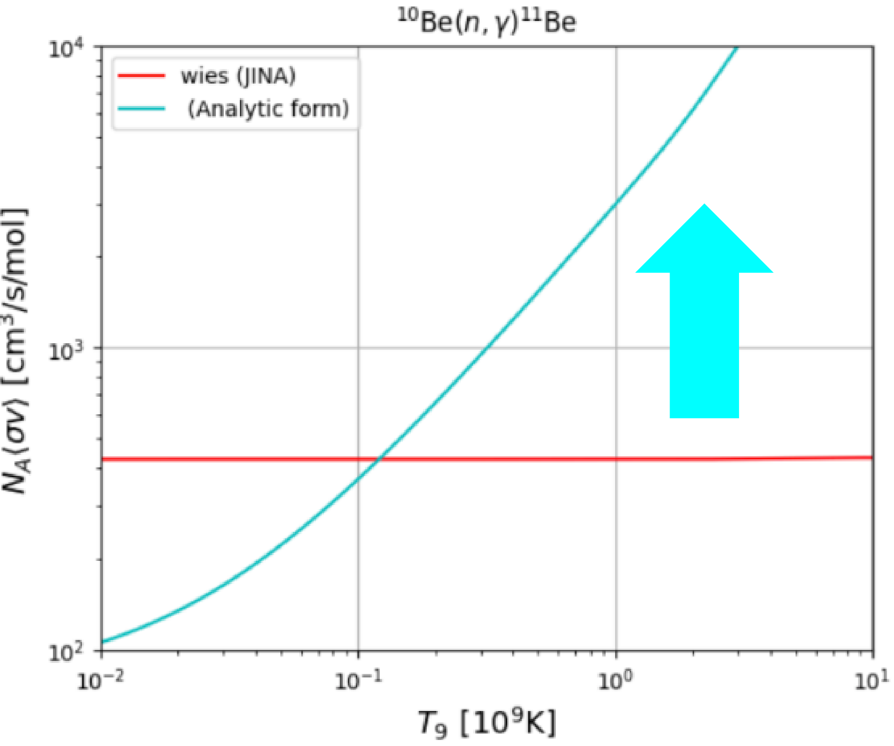

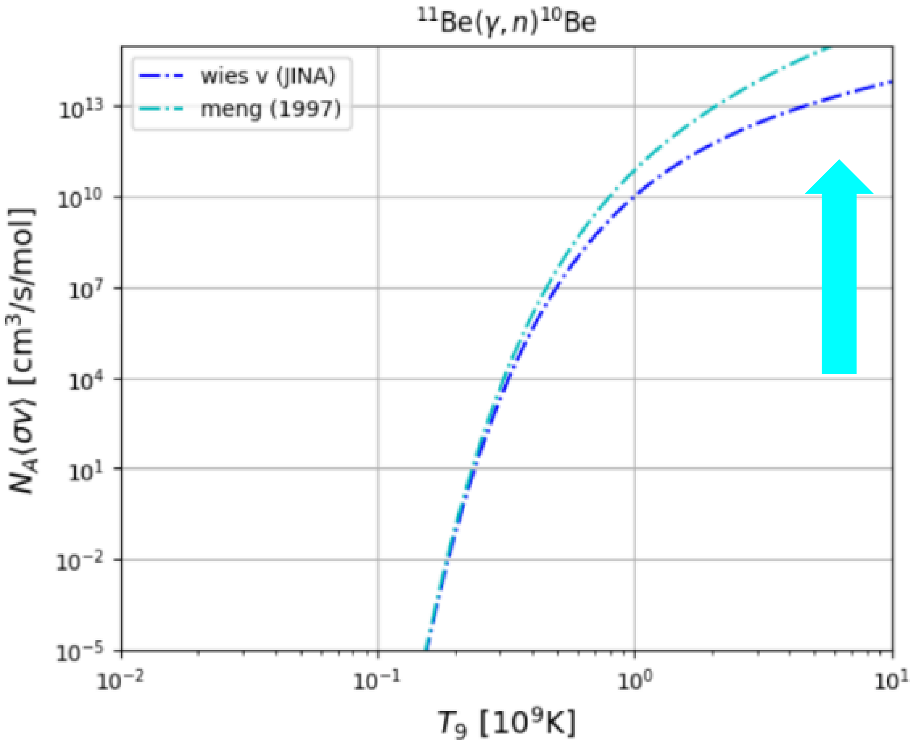

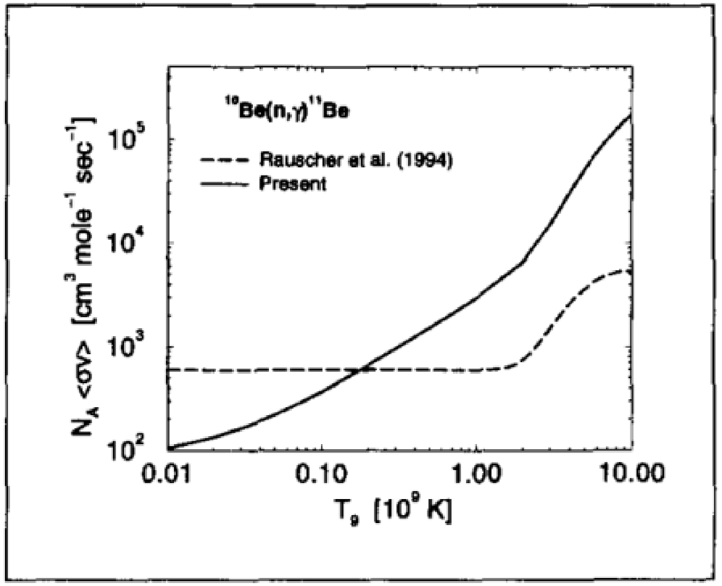

A. Mengoni et al. Nuclear Physics A621 (1997)

4. $^{10}Be(n,\gamma)^{11}Be$ Q-value = 0.504369 MeV

- wies (**JINA**) - various refs. M. wiescher (2000)
- Halo state (A. Mengoni et al. (1997)

-> We follow the equation in the paper rather above figure

At the final result...

1. $^{10}Be(p,n)^{10}B$ Q-value = -0.22559 MeV
   - mk16 - TALYS-1.8 code (2015)
   - sc22 - S. Chiba (g.s. from JENDL-5.0)
   - jl23 - by Dr. Lee

2. $^{10}Be(p,\alpha)^{7}Li$ Q-value = 2.56411 MeV
   - wagn (JINA) - R.V. Wagoner APJsup (1969)
   - Sensitivity study (Severing et al. (2022)

3. $^{10}Be(\alpha,n)^{13}C$ Q-value = 3.83555 MeV
   - wiesr (JINA) - various refs. M. wiescher (2000)
     resonate rate
   - JENDL-5 ($^{13}C(n,\alpha)^{10}Be$ reaction cross section)

4. $^{10}Be(n,\gamma)^{11}Be$ Q-value = 0.504369 MeV
   - wies (JINA) - various refs. M. wiescher (2000)
   - Halo state (A. Mengoni et al. (1997) (Analytic form)

As the final result, we selected each pink color case.

At the final result…

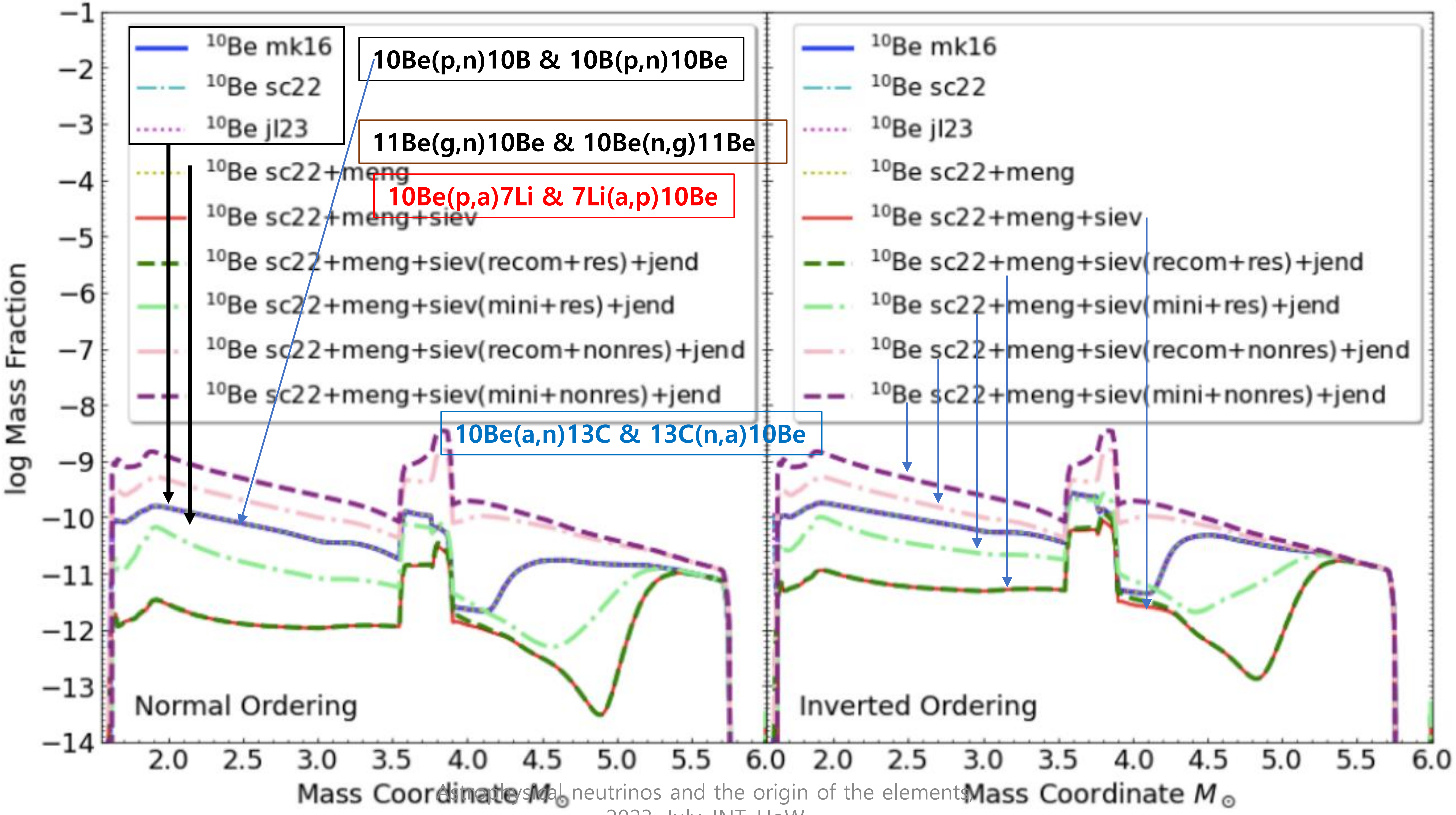

At the final result bar graph

For the case all included (sc22+meng+siev(recom+res)+jend)

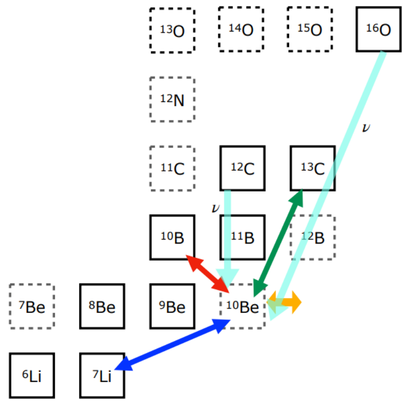

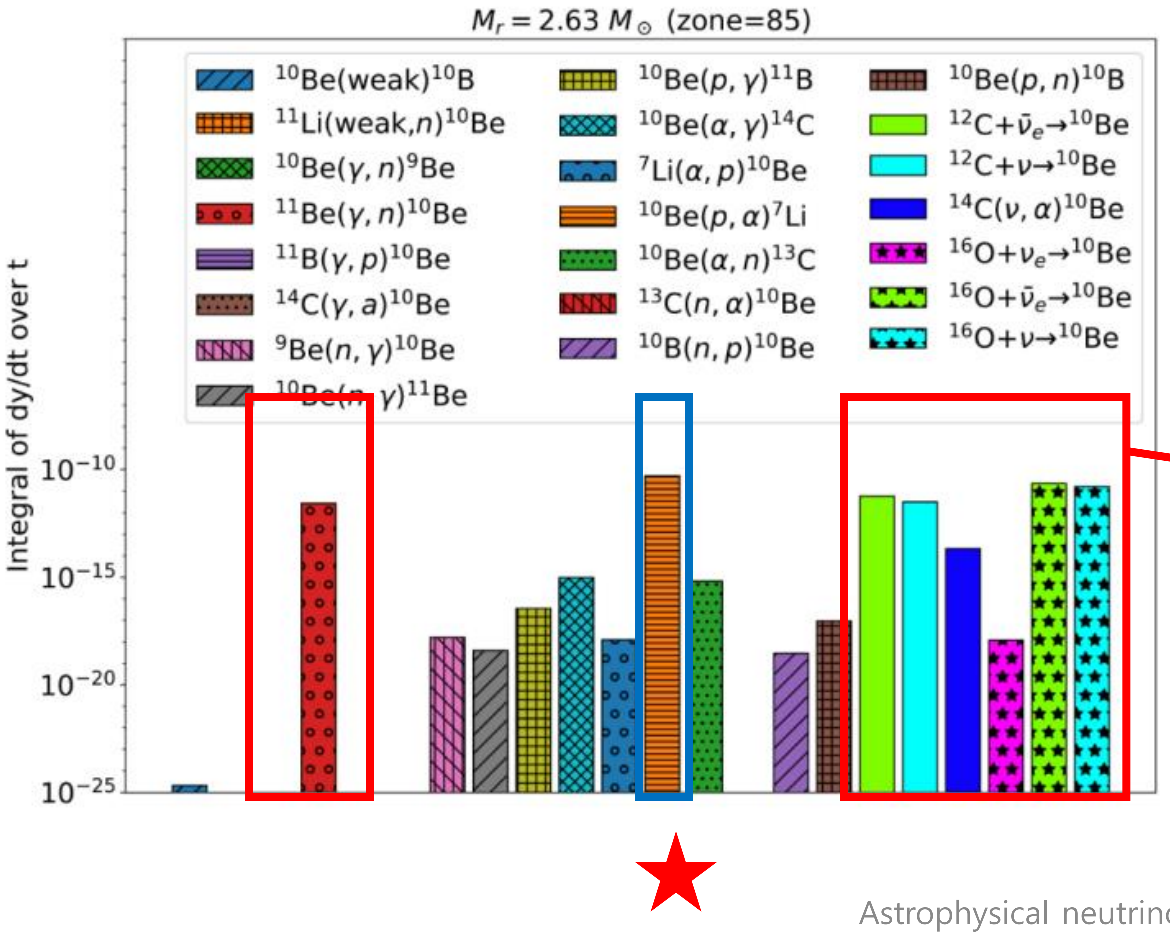

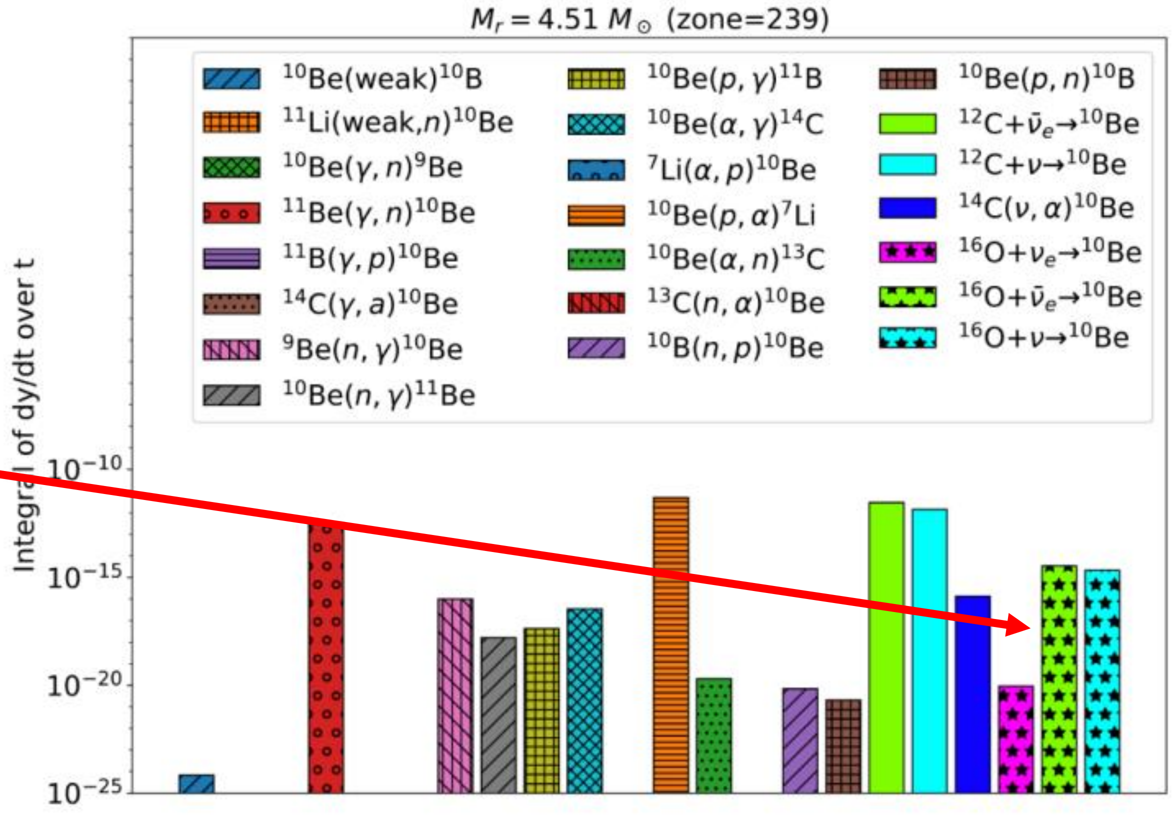

The integrated mass of ^{10}Be

naming	Normal Ordering (10^{-10} M_{sun})	Inverted Ordering (10^{-10} M_{sun})	Type
mk16	1.939	2.911	8/9 (mod)
jl23	1.944	2.923	10/11
sc22	1.944	2.923	12/13
sc22+meng	1.944	2.916	14/15
sc22+meng+siev	0.1397	0.4184	16/17
sc22+meng+siev(recom+res) +jend	0.1453	0.4635	18/19
sc22+meng+siev(mini+res) +jend	0.6812	1.575	20/21
sc22+meng+siev(recom+ nonres)+jend	4.810	7.411	18_1/19_1
sc22+meng+siev(mini+ nonres)+jend	13.36	17.48	20_1/21_1

Mass fraction ratio of $^{10}Be/^{9}Be$

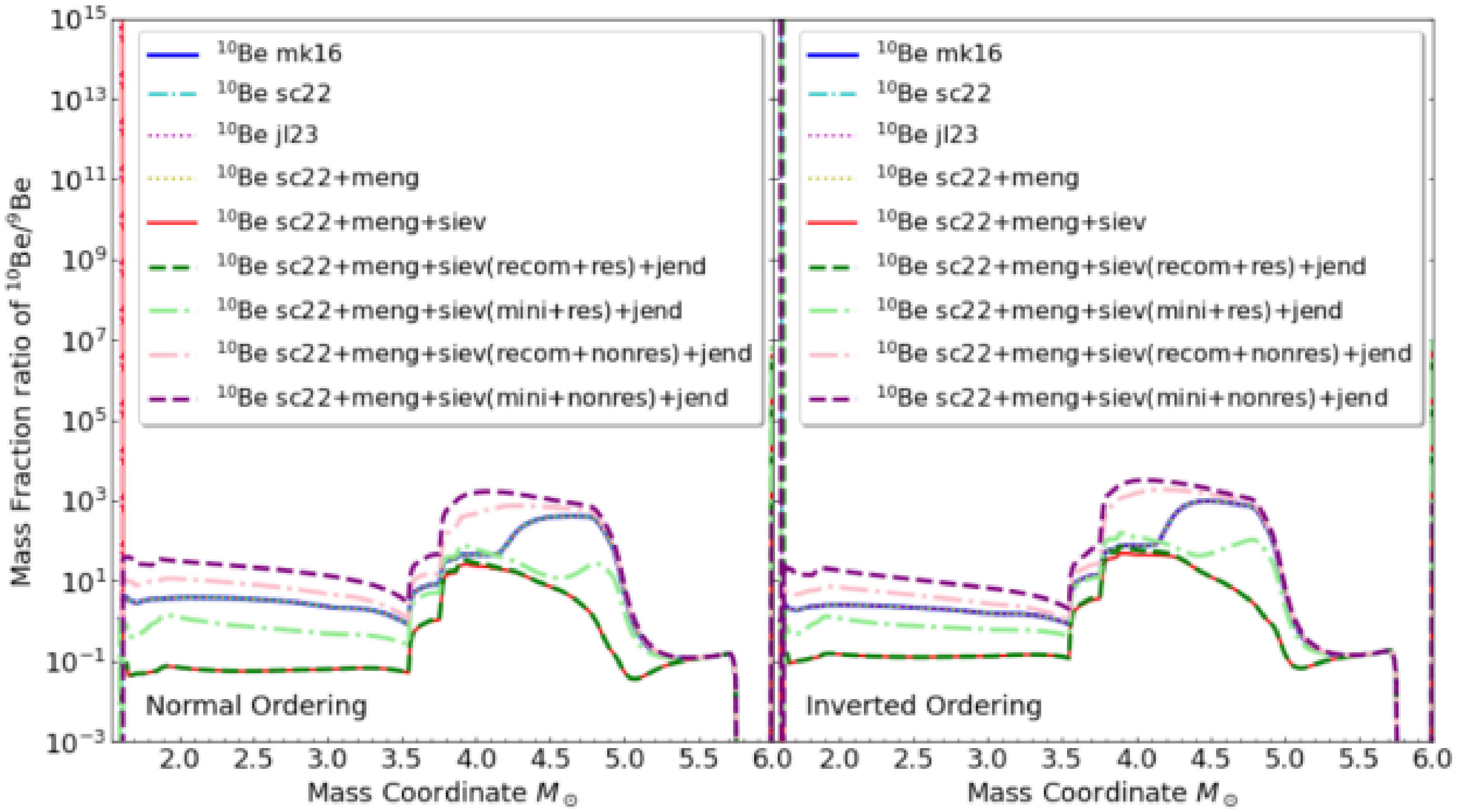

The ratio

- At 50 s

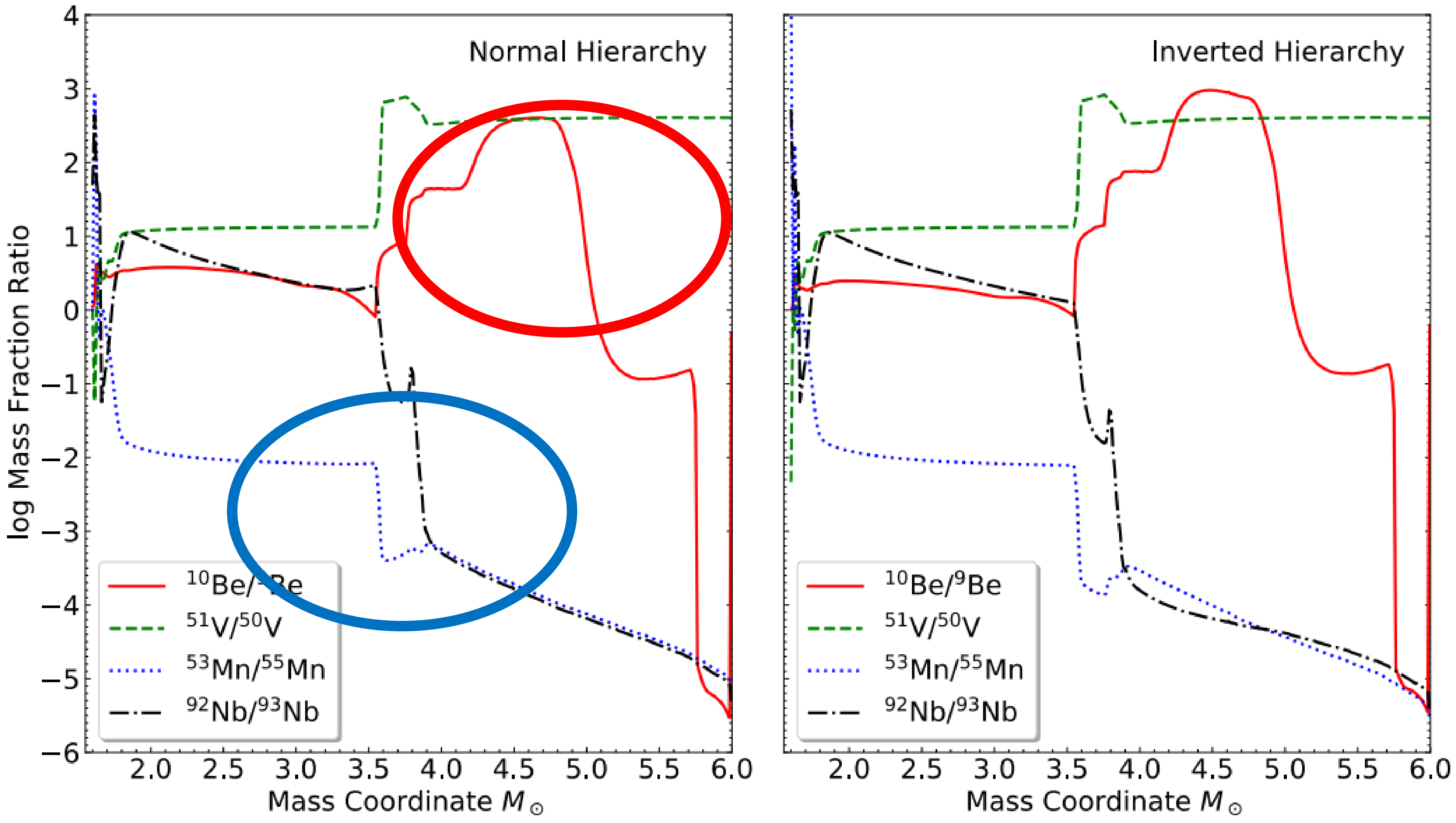

존재비 (NNDC 데이터)

^{9}Be(100%)
^{51}V (99.75%) and ^{50}V (0.25%)
^{55}Mn(100%)
^{93}Nb(100%)

Integrated mass $M_\odot$ (NH)

^{9}Be(1.116E-10) and ^{10}Be(1.939E-10)
^{51}V (3.610E-07) and ^{50}V (9.044E-08)
^{53}Mn(2.674E-05) and ^{55}Mn(1.052E-05)
^{92}Nb(4.612E-12) and ^{93}Nb(8.006E-10)

4. Summary and Conclusion

1. We updated the nuclear reactions relevant to the production and destruction channels for 10Be.

2. Main production reactions are found to be neutrino-induced reactions on 12C and 16O as well as 11Be(γ, n)10Be, while the main destruction channel is shown to be 10Be(p,α)7Li.

3. The charge exchange reactions are shown to rarely contribute the 10Be production.

4. The 10Be abundance is shown to reach to 0.14 – 0.68 for normal hierarchy and 0.46 – 1.57 for inverse hierarchy in the unit of [$10^{-10} M_\odot$], if we take into account of the resonance 1/2+ at E_ex=11.425 MeV in 11B produced by radiative proton capture.

5. This abundance is a bit smaller than the previous result 3.26 [$10^{-10} M_\odot$] by A. Heger because of the resonance in 11B created the destruction channel 10Be(p,α) 7Li.

6. We also presented the evolution of the abundance ratio of 10Be to 9Be with the mass coordinate in the supernova.

7. Similar calculations of other short lived radioactive nuclei, 51V and 53Mn, have been done and will be analyzed for the SN event near the solar system formation by comparing their ratios to their stable isotopes 10Be/9Be, 51V/50V, 53Mn/55Mn, and 92Nb/93Nb.

8. We included the neutrino self interaction, which is slow flavor oscillation effect, using the bulb model, the multi-angle approximation in the present calculation and the empirical neutrino distribution by Fogli.

9. The fast flavor instability also change the neutrino spectra and will be considered as a future project. But we need numerical results.

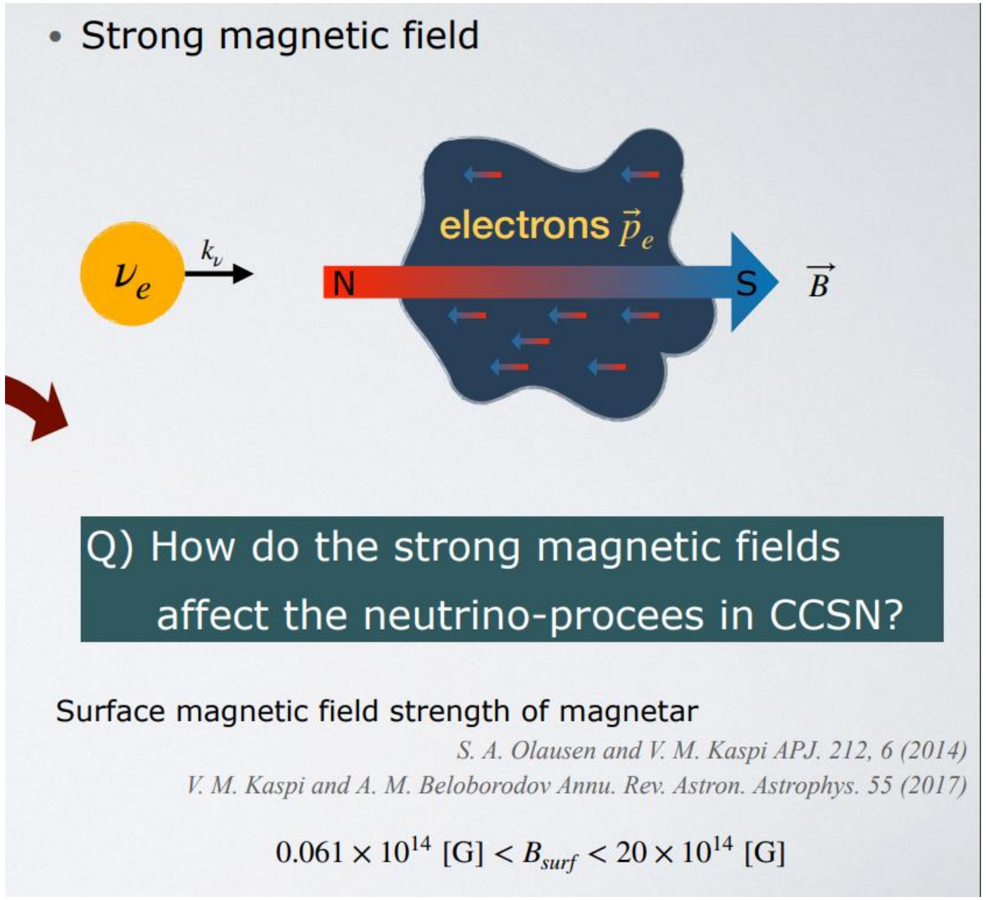

10. As for the magnetic field effect, we recently considered first the electron polarization in the pre-SN matter before the magnetic field effect in the neutrino transport inside the proto-neutron star.

11. Finally, we are going to develop the Late Input Model for understanding of the last SN around the solar system formation with help of the meteorite analyses. They now evaluate which shell the SLR nuclei are produced in the CCSNe.

The first University in Korea
Soongsil University

Thanks for your attention !!

OMEG
Origin of Matter and Evolution of Galaxies
Key Research Institutes in Universities